Received: 5 January 2022 | Revised: 26 April 2022 | Accepted: 26 April 2022

DOI: 10.1111/joa.13686

Journal of Anatomy ANATOMICAL SOCIETY WILEY

ORIGINAL PAPER

Developmental stages of the ballan wrasse from first feeding through metamorphosis: Cranial ossification and the digestive system

Sissel Norland[1] | Øystein Sæle[2] | Ivar Rønnestad[1]

[1]Department of Biological Sciences, University of Bergen, Bergen, Norway

[2]National Institute of Nutrition and Seafood Research, Bergen, Norway

Correspondence
Øystein Sæle, National Institute of Nutrition and Seafood Research, P.O. Box. 2029 Nordnes, 5817 Bergen, Norway.
Email: oystein.saele@hi.no

Ivar Rønnestad, Department of Biological Sciences, University of Bergen, P.O. Box 7800, 5020 Bergen, Norway.
Email: ivar.ronnestad@uib.no

Funding information
Norges Forskningsråd, Grant/Award Number: 244170 311627; L. Meltzers Høyskolefond, Grant/Award Number: Sabbatical grants to IR

Abstract

We have described six developmental stages for the ballan wrasse, from the first feeding until the juvenile stage, supported by specific descriptions of cranial ossification, maturation of the digestive tract, and growth-correlated stages. The initial formation and development of bones are closely linked to the functional anatomical structures required for the mechanics of its feeding behavior and ingestion, particularly the jaws and branchial regions involved in opening the mouth and capturing food particles. The overall ontogeny of the cranial structure compares to that of other teleosts. The cranial ossification of the ballan wrasse skull and the development of its dentary apparatus—first pharyngal teeth and later oral teeth—is linked to the development of the digestive system and to their feeding habits, from preying on zooplankton to feeding on crustaceans and invertebrates on rocks and other substrates. As ballan wrasse is a nibbler, eating small meals, the digestive tract is short compared to the length of the fish; there is no stomach or peptic digestion and also no distinctive bulbus and pyloric ceca. The liver and exocrine pancreas and their outlets terminating in the lumen of the most anterior part of the intestine are important in the digestive process and develop with a larger volume than that in gastric teleosts, relative to the digestive system.

KEYWORDS
agastric, cranium, development, digestion, feeding, intestine, jaws, marine fish larva

1 | INTRODUCTION

The ballan wrasse (*Labrus bergylta*) is an important species in aquaculture, being used as a cleaner fish, grazing upon sea lice on farmed Atlantic salmon (*Salmo salar*; Bjordal, 1988, Ottesen et al., 2008, Skiftesvik et al., 2013). To avoid overfishing of wild wrasse populations, and to provide a supply for the increasing demands for wrasse in the salmon industry, commercial production of farm wrasses has been established (Costello, 2006; Hamre, Nordgreen, et al., 2013; Skiftesvik et al., 2013). However, the industry is relatively new and knowledge of several key aspects of the feeding biology of ballan wrasse is limited; this continues to pose challenges compared to other cleaner fish species already established in the industry. It is thus essential to understand the functional development and physiological responses in traits that are critical to the successful capture and digestion of food, particularly in the early stages of ballan wrasse development.

Fish ontogeny includes periods of allometric growth when different organs and organ systems develop at different rates.

The head and tail of fish larvae develop first, which is advantageous for feeding, locomotion, and escape behavior (Osse & van den Boogaart, 1995; Yúfera & Darías, 2007). A range of transformations occurs as organs become functional and mature. These include development and reorganization of the digestive system with accessory organs (Marques et al., 2017); skeletal muscles (Yamano et al., 1991); oxygen delivery systems including gills, circulatory system, and erythrocyte maturation with the appearance of hemoglobin (Burggren & Pinder, 1991; Inui et al., 1995); and sensory structures such as the eyes with alteration of photoreceptor composition (Valen et al., 2016). There are, however, species-specific differences in timing, characteristics, and adaptations in the morphology and physiology of organs and organ systems during development. Prior to the onset of exogenous feeding, throughout the larval period and juvenile metamorphosis in marine fish, the larval digestive system undergoes significant morphological, physiological, and functional change (Rønnestad et al., 2013; Wallace et al., 2005; Yúfera & Darías, 2007; Zambonino Infante et al., 2008).

When describing and comparing the development of fish larvae, particularly when describing a wide range of functional attributes related to aquaculture, it is common to refer to the age of the fish in terms of days post-fertilization (dpf) or days post-hatching (dph). However, studies have repeatedly shown that age alone is a poor descriptor of developing larvae (Sæle & Pittman, 2010), particularly since developmental rates depend strongly on temperature. Similarly, using fish length as an indicator of development poses its own problem: length is an incomplete characterization of larval development since larvae display allometric growth (Heath, 1992). An alternative is to characterize larval development into stages, with a detailed description of the externally visible anatomy of the living fish, including size (Parichy et al., 2009) combined with such additional characteristics as bone development, cranial ossification, and myotome height (MH) (Sæle & Pittman, 2010). On this basis, a staging series with defined developmental stages and milestones based on cranial ossification has been established for the Atlantic cod *Gadus morhua* (Sæle et al., 2017) and Atlantic halibut *Hippoglossus hippoglossus* (Sæle et al., 2004). There are currently no guidelines for the classification of larval development and defined ontogenetic stages for the ballan wrasse, except for an applied and commercially useful categorization proposed by Ottesen et al. (2012). These authors defined four developmental stages based on standard length (SL) and outer morphology of ballan wrasse larvae. We propose an extended categorization of developmental stages in ballan wrasse supported by ossification of cranial bones in combination with defined milestones and ontogeny of the digestive system.

The initial formation and development of bones are closely linked to the functional anatomical structures required for the mechanics of feeding behavior and ingestion, particularly the jaws and branchial regions involved in opening the mouth and capturing food particles. This includes the hyoid and branchial arches, as well as the neurocranium, jaws, suspensorium, and opercular. The formation process includes chondrification, forming cartilage, and ossification, forming bone. The overall ontogeny of the cranial structure is highly conserved in teleosts (Faustino & Power, 2001). Knowledge of the normal ossification sequence of bones can assist in recognizing skeletal deformities caused, for instance, by inadequate nutrition (Hamre, Yúfera, et al., 2013; Sæle et al., 2003; Sæle et al., 2017); such knowledge can also contribute to identify the underlying cause and rectifying the problems.

There are nearly 30,000 species of teleosts that inhabit all imaginable niches in the aqueous environment. The specialization of feeding among fish is reflected in how the digestive apparatus, starting with the jaws, the stomach (when present), and the intestine. While some species hatch small offspring that look like adults and already possess teeth in the jaw and a functional stomach, many other species hatch relatively primitive translucent larvae with a short intestine without a functional stomach. This latter type of larvae are specialized pelagic plankton feeders that will eventually undergo metamorphosis, transforming into its adult form—which is usually adapted to a different habitat and diet: for example, Atlantic cod (Kamisaka & Rønnestad, 2011) and Atlantic halibut (Gomes et al., 2014).

Although useful, a functional stomach is not required for all feeding habits. A stomach requires energy to synthesize and maintain function; accordingly, the stomach has been independently lost 15 times in the teleost evolution (Castro et al., 2014). One example of an agastric species—that is, having no functional stomach—is ballan wrasse. The agastric fishes have lost protein digestion related to stomach function—pepsin and proton-pump capacity (Castro et al., 2014; Lie et al., 2018)—and variations in the digestive tract often reflect their feeding habits and food preferences regardless of the presence or absence of a functional stomach (Ray & Ringø, 2014).

Like all fish that lack a stomach, the ballan wrasse also lacks pyloric ceca, and the digestive tract in this species is also relatively short compared to the length of the fish. The stomach in gastric species serves a range of physiological purposes, including (a) short-term food storage, (b) digestion of proteins, (c) gradual and controlled delivery of chyme to the anterior intestine to optimize further processing (digestion and absorption), (d) osmoregulatory function, and (e) acting as a barrier against pathogens (Koelz, 2009; Rønnestad et al., 2013). Several studies support the idea that agastric fishes have some ability to retain food in the anterior part of the intestine, sometimes visible as a bulb. However, we have recently shown that the anterior part of the ballan wrasse gut does not have any special function of storage or retention of ingested food while waiting for the main digestion (Le, Shao, et al., 2019). Up to 70% of nutrients were digested and absorbed in the anterior intestine, and the rest of the digesta was propelled backward only a few hours post-ingestion. The feeding ballan wrasse is a nibbler, eating frequent small meals, and therefore does not need to store food in a special compartment for subsequent digestion (Le, Shao, et al., 2019).

For agastric fish larva to digest complex proteins without the contribution of pepsin and acid secretion in the stomach, secretion of enzymes from the exocrine pancreas play a key role in proteolysis

(Gomes et al., 2014; Hansen et al., 2013; Rønnestad et al., 2007). In agastric species, the feed particles move directly from the esophagus to the intestine (Smith et al., 2000) at the site where the common bile duct and pancreatic duct terminate in the lumen of the intestine. If the ingested food enters a functional bulbus at the site where bile and pancreatic secretions are released, this will help to efficiently mix the food with digestive enzymes to improve digestion rates and absorption.

In this paper, we propose an extensive categorization of developmental stages in ballan wrasse from first-feeding larvae to the juvenile phase, in accordance with and comparable to the defined developmental stages for Atlantic cod (Sæle et al., 2017) and Atlantic halibut (Sæle et al., 2004). The staging description was based on two experiments. The first experiment was used to define the developmental stages, including the description of standard length (SL) and myotome height (MH), by correlating ossification of the cranium. The second experiment described the ontogeny of the digestive system and proposed processing capacity in terms of morphometric scaling, and how it changes during development according to the developmental stages established in experiment 1. To facilitate the conceptualization of the spatial distribution and orientation of the digestive organs, we developed a three-dimensional representation of the digestive organs similar to that previously developed for visualization of the ontogeny of the digestive system of Atlantic cod (Kamisaka & Rønnestad, 2011) and Atlantic halibut (Gomes et al., 2014). 3D rendering of the digestive system permits rotating and zooming the model from all angles while adding or hiding organs in studies of the exterior and interior surfaces. The present study extends the work of Kamisaka and Rønnestad (2011) and Gomes et al. (2014) to the ballan wrasse to better understand the development of its functional gut anatomy, including details of organ shape, size, and relative position at different developmental stages.

Collectively, we propose developmental stages in ballan wrasse from first-feeding larvae through metamorphosis based on SL, MH, cranial-bone ontogenesis, and ossification together with the maturation of the digestive system.

2 | MATERIALS AND METHODS

2.1 | Ethical statement

Sampling for both trials was conducted at a commercial hatchery (Marine Harvest Labrus; now Mowi, Rong, Norway) where ballan wrasse was reared in accordance with the Norwegian Animal Welfare Act of December 12, 1974, no. 73, sections 22 and 30, amended June 19, 2009. The facility has a general permission to rear all developmental stages of *L. bergylta*, license number H ØN0038 provided by the Norwegian Directorate of Fisheries (https://www.fiskeridir.no/English).

Since fish were sampled from the normal production line and did not undergo any treatment or handling except for euthanasia, a special approval from the food authorities and ethics committee was deemed unnecessary according to Norwegian regulations "Legislation on the use of animals," section 6: "Approval of study" (English translation from https://lovdata.no). Section 6 states that the need for approval does not apply to studies that only use animals for their organs or tissues. All fish used were euthanized with an overdose of metacaine (MS-222TM; Norsk Medisinaldepot AS) on site, before fixation.

2.2 | Rearing conditions

Two batches of fertilized eggs (collected on August 21–22 and 27–28, 2015) were obtained from natural spawning fish distributed into eight tanks (~9000 L), each containing 30 females and five males. The collected eggs were incubated in 900–1000 L tanks for 9 days at 11.3°C, 12/12 h light/dark regime until hatching. Newly hatched larvae (0 dph) were transferred to feeding tanks (9000 L; initial stock density 1.0–1.3 × 10^6 larvae, 13.7°C, water flow 45 L/min). Larvae were kept under 24 h darkness until 4 dph. From 4 dph, the larvae were kept under a 24 h light regime and fed four times daily. Water flow and temperature were gradually increased to 60 L/min at 22 dph and 16°C at 24 dph, respectively. Rotifers (*Brachionus* spp., Aquafarms) and *Artemia* spp. (INVE Aquaculture Inc.), both enriched with Multigrain (BioMar), were given as live feed to the larvae from 4–25 to 25–57 dph, respectively (for rotifer and *Artemia* production, see Data S1). A co-feeding protocol (live *Artemia* and formulated feed; Nofima) was introduced at 47 dph and kept for 10 days. The larvae were fed only formulated feed from 57 dph (Otohime B1/B2 and later C1).

2.3 | Biological sampling

2.3.1 | Experiment 1: Defining developmental stages by morphometrics and bone-staining observations

Five wrasse larvae from each tank were collected at 2, 5, 8, 9, 12, 13, 16, 17, 20, 24, 27, 31, 32, 35, 38, 44, 46, 49, 52, 58, 61, 65, 72, and 79 days post-fertilization (dpf) for skeletal analysis. Shortly after sampling, the larvae were sedated (metacaine) and visually examined for quality under a microscope (including signs of abnormal development, injuries, or diseases), photographed to determine SL and MH using ImageJ (NIH), then fixed with 10% buffered formalin. Staining with alizarin red S was performed according to the following procedure described by Sæle et al. (2003): Three-hour immersion in a 0.1 M NaOH, containing 0.18% alizarin red ($C_{14}H_7O_7SNa$; Merck), was followed by washing four times, each for 30 min, in distilled water. Thereafter, the larvae were dehydrated in 70% ethanol overnight, followed by dehydration in 90% ethanol for 1 h. Larvae were preserved and cleared in 87% glycerol (Merck). Alizarin red combines with calcium (bone is a calcified tissue matrix) and is visualized as red/orange in calcified areas (Potthoff, 1984).

TABLE 1 Sequence of ossification in ballan wrasse from 2 to 79 days post-hatching (dph). Each column represents an individual larva. Rows indicate the scores for individual bone. For bones of which there are several of the same type, the quantity of the specific type of bones is given in parentheses

Age (dpsf)		2	2	5	5	5	5	8	8	9	9	12	12	16	9	12	12	13	20	16	16	20	13	17	20	27	24
Premaxillary	*Pmax*																					1	1	1	1	1	2
Maxillary	*Max*																	1		1	1	1	1	1	1	2	2
Palatinum	*Pal*																										
Mesopterygoid	*Mpt*																										
Entopterygoid	*Enpt*																										
Ectopterygoid	*Ecpt*																										
Quadrate	*Quad*																										
Articular	*Ar*																									1	1
Angular	*An*																										
Dentary	*Den*																			1	1	1	1	1	1	2	2
Hyoid arch																											
Hyomandibular	*Hyo*																										
Symplecticum	*Spl*																										
Interhyal	*Ihy*																										
Epihyal	*Ehy*																										
Ceratohyal	*Chy*																									1	1
Hypohyal	*Hhy*																										
Basihyal	*Bhy*																										
Urohyal	*Uhy*																										
Glossohyal	*Ghy*																										
Operculum																											
Operculum	*Op*														1						1	1	1	1	1	1	1
Praeoperculum	*Pop*																									1	1
Suboperculum	*Sop*																									1	1
Interoperculum	*Iop*																										1
Neurocranium																											
Nasal	*Nas*																										
Ethmoid group	*Eth*																										
Lacrymal	*Lac*																										
Frontal	*Fro*																										
Parietal	*Par*																										
Vomer	*Vo*																									1	
Parasphenoid	*Psp*																						1	1		1	1
Basispheniod	*Bsp*																										1
Pterosphenoid	*Ptsp*																										
Pteroticum	*Pot*																										
Sphenoticum	*Sph*																										
Epioticum	*Eot*																										
Prooticum	*Oot*																										
Supraoccipital	*Socc*																										
Exoccipital	*Eocc*																									1	1
Basioccipital	*Bocc*																									1	1
Circumorbital	*Corb*																										
Branciales																											
Pharyngobranchial	*Pbra*																										
Epibranchial	*Ebra*																										
Ceratobranchial	*Cbra*																									1(4)	1(4)
Hypobranchial	*Hbra*																										
Basibranchial	*Bbra*																										
Dorsal pharyngeal teeth	*Dpt*															1	1	1	1	1	1	1	1	1	2	2	2
Ventral pharyngeal teeth	*Vpt*																1		1	1	1	1	1	1	2	2	2
Score		0	0	0	0	0	0	0	0	0	0	0	0	0	1	1	2	2	2	4	5	6	7	7	8	19	21

Note: (1) presence of mineralization in bone; (2) establishment of a distinctive bone shape; (3) bone with a shape like that in adults.
Abbreviation: dph, days post-hatching.

24	31	38	32	35	44	32	44	49	52	49	52	46	61	58	65	72	61	65	75	72	65	75	75	79	79
2	2	2	2	2	2	2	2	2	2	2	2	3	2	3	3	3	3	3	3	3	3	3	3	3	3
1	2	2	2	2	2	2	2	2	2	2	2	3	2	3	3	3	3	3	3	3	3	3	3	3	3
						1	2	2	2	2	2	2	2	2	2	2	3	2	3	3	3	3	3	3	3
							1	1	2	1	2	2	2	2	2	2	2	2	2	2	2	3	2	3	
			1	1		1	1	1	2	1	2	2	2	2	2	2	2	2	2	2	2	3	3	3	
		1	1	1	1	1	2	2	2	2	2	2	2	2	2	2	2	2	2	3	3	3	3	3	
1	1	1	2	1	2	2	2	2	2	1	2	2	2	2	2	2	2	2	2	2	3	3	3	3	
1	1	1	2	2	2	2	2	2	2	1	2	3	2	3	3	3	3	3	3	3	3	3	3	3	
1	1	1	2	2	2	2	2	2	2	2	3	3	3	3	3	3	3	3	3	3	3	3	3	3	
2	2	2	2	2	2	2	2	2	2	2	2	3	2	3	3	3	3	3	3	3	3	3	3	3	

1	1	2	2	2	2	2	2	2	2	2	2	2	2	3	2	3	3	3	3	3	3	3	3	3	
1	1	1	2	2	1	2	2	2	2	1	2	2	2	2	2	2	2	2	2	3	3	3	3	3	
			1	2	2	2	2	2	2	2	2	2	3	3	3	3	3	3	3	3	3	3	3	3	
			1	2	2	2	2	2	2	2	2	3	3	3	3	3	3	3	3	3	3	3	3	3	
1	1	1	2	2	2	2	2	2	2	2	2	3	3	3	3	3	3	3	3	3	3	3	3	3	
			1		2	2	2	1	1	2	2	2	3	3	3	3	3	3	3	3	3	3	3	3	
			1	1	2	2	2	1	1	2	2	2	2	2	3	3	2	3	3	3	3	3	3	3	
			1	1	2	2	2	2	1	2	2	2	2	2	2	2	3	2	3	3	3	3	3	3	
					1	1	2	1	1	1	2	2	2	2	2	2	2	2	3	3	3	3	3	3	

1	1	2	2	2	2	2	2	2	2	2	2	2	3	3	3	3	3	3	3	3	3	3	3	3	
1	1	2	2	2	2	2	2	2	2	2	2	2	3	3	3	3	3	3	3	3	3	3	3	3	
1	1	2	2	2	2	2	2	2	2	2	2	2	2	2	2	2	2	3	3	2	3	3	3	3	
1	1	2	2	2	2	2	2	2	2	2	2	3	3	3	3	3	3	3	3	3	3	3	3	3	

				1		1	1		1		1	2	2	2	2	1	2	2	2	2	2	3	3	3	
												1	1	1	1	1	1	1	1	1	2	2	2	3	
			1	1	1	2	2	2	2	2	1	2	2	2	2	2	2	2	2	2	2	2	2	2	
		1	1	1	1	1	1	1	1	1	1	2	2	2	2	2	2	2	2	2	2	2	2	2	
			1	1		1	1	1	1	1	1	2	2	2	2	2	2	2	2	3	2	3	3	3	
			1	1		1	1	1	1	1	1	2	2	1	2	2	2	3	3	2	3	3	3	3	
1	2	2	2	2	2	2	2	2	2	2	2	2	3	3	3	3	3	3	3	3	3	3	3	3	
1	2	2	2	1	2	2	2	2	2	2	2	2	3	2	3	3	3	3	3	3	3	3	3	3	
		1	1	1	1	1	1	2	2	2	2	2	2	2	2	2	2	3	3	2	3	3	3	3	
	1	1	1	1	1	1	1	2	2	2	2	2	2	2	2	2	2	3	3	3	3	3	3	3	
			1	1	1	1	1	2	2	2	2	2	2	2	2	2	2	3	3	2	3	3	3	3	
			1	1	1	1	1	2	2	2	2	2	2	2	2	2	2	3	2	3	3	3	3	3	
1	1	1	1	1	1	1	1	2	2	2	2	2	2	2	2	2	2	3	3	3	3	3	3	3	
			1	1	1	1	1	2	1	2	1	2	2	2	2	2	2	2	3	3	2	3	3	3	
1	1	2	2	2	2	2	2	2	2	2	2	2	3	3	3	3	3	3	3	3	3	3	3	3	
1	2	2	2	2	2	2	2	2	2	2	2	2	3	3	3	3	3	3	3	3	3	3	3	3	
													1		1		1	1	2	1	2	2	2	3	3

					1(4)		2(4)	1(4)	1(4)	2(4)	2(4)	2(4)	2(4)	2(4)	2(4)	2(4)	2(4)	2(4)	3(4)	3(4)	3(4)	3(4)	3(4)	3(4)	3(4)
			1(2)	1(4)	1(4)	1(2)	2(4)	2(4)	2(4)	2(4)	2(4)	2(4)	2(4)	2(4)	2(4)	2(4)	2(4)	2(4)	3(4)	3(4)	3(4)	3(4)	3(4)	3(4)	3(4)
1(4)	1(4)	1(4)	1(4)	2(4)	1(4)	1(4)	2(4)	2(4)	2(4)	2(4)	2(4)	2(4)	2(4)	2(4)	2(4)	2(4)	2(4)	2(4)	2(4)	3(4)	3(4)	3(4)	3(4)	3(4)	3(4)
				1(3)	1(3)		1(3)	1(3)	1(2)	1(3)	2(3)	2(3)	2(3)	2(3)	2(3)	2(3)	2(3)	2(3)	2(3)	3(3)	3(4)	3(3)	3(3)	3(4)	3(4)
				1	1		1	1	1	1	1	2	2	1	2	2	2	2	2	3	3	3	3	3	3
2	2	2	2	2	2	2	2	2	2	3	3	3	3	3	3	3	3	3	3	3	3	3	3	3	
2	2	2	2	2	2	2	2	2	2	3	3	3	3	3	3	3	3	3	3	3	3	3	3	3	
25	30	39	57	60	62	64	76	77	78	79	86	101	106	107	110	110	113	119	125	127	132	134	137	137	139

2.3.2 | Experiment 2: Ontogeny of the digestive system

Based on the results of Experiment 1 for the characteristics and SL defining the six developmental stages, larvae were sampled at 4, 10, 18, 29, 71, and 102 dph for stages 1–6, respectively, for the stage-specific description of the developmental status of the digestive system. Great care was taken to select larvae that fitted the typical characterization for each stage, based on SL and outer characteristics (including yolk sac consumption, skin pigmentation, and fin development) from Experiment 1. Shortly after sampling, the larvae were sedated (metacaine) and examined for quality under a microscope and photographed to determine SL measurement (ImageJ), whole larvae were fixed by immersion in a mixture of 2% PF, 2.5% glutaraldehyde, 40 mM cacodylate buffer and 1× PBS and then stored in 70% ethanol.

2.4 | Confocal microscopy

Confocal microscopy of alizarin red-stained larval teeth was performed using an inverted microscope (Ti; Nikon) with a C2+ confocal scanner (Nikon) and the following scanner settings: first filter cube, 447/60; second filter cube, 525/50561 LP; emission wavelength, 785 nm; laser power, 3.4; and pinhole size, 30 μm^2.

2.5 | Scanning electron microscopy

Two fixed larvae from each stage were dissected using razor blades and rehydrated (70%–50% ethanol) prior to secondary fixation in 1% osmium tetroxide (OsO_4; Merck KGaA) for 1 h. After the secondary fixation, the larvae were rinsed in distilled water and dehydrated (50%–70%–96%–100% acetone series) before critical-point drying. Larvae were sputter-coated with gold–palladium using a Polaron SC502 Sputter Coater (Quorum Technologies) and examined using a ZEISS Supra 5VP field-emission scanning electron microscope. The size of the enterocytes was examined in ImageJ (https://imagej.net/, RRID:SCR_003070).

2.6 | Light microscopy and 3D reconstructions of the digestive organs

One high-quality larva from each stage (stages 1–6) was carefully selected and prepared for light microscopy. The larvae were dehydrated in 96% ethanol (2 × 15 min), embedded in Technovit 7100 (Heraeus Kulzer GmbH), and cut into semi-thin (2 μm) longitudinal serial sections. The sections were stained with toluidine blue and scanned using an RS Photometrics CoolSNAP-PRO camera mounted on either a Leica M420 macroscope with a 6:1 Leica Apozoom objective or on a Leica DMLB microscope.

Every 2nd (for stage 1) to 13th (for the remaining stages) sections were used for 3D reconstructions. Micrographs were edited in Adobe Photoshop CC2015 (Adobe System Inc., USA, RRID:SCR_014199), batch converted, and renamed using IrfanView (http://www.irfanview.com/, RRID:SCR_000315). Alignment of image stacks was performed in AutoAligner 6.1 (Bitplane AG, RRID:SCR_007355). Aligned image stacks were uploaded into Imaris 8.4 (Bitplane AG, RRID:SCR_007370) for 3D reconstruction. One 3D model was created for each stage, consisting of the digestive tract from the pharynx to the anus, and associated organs or tissues (liver, pancreas, and gallbladder) observed at the given stage. Each observed tissue or organ was manually drawn as node polygons with a specific color code for the specific surface (e.g., the liver for all stages was red). For further details on the method used for 3D reconstruction, see Data S2.

Complete drawn surfaces were 3D reconstructed using the Imaris software. Screenshots with different transparencies for each layer were used to document the 3D models for each developmental stage. Imaris MeasurementPro (extension of Imaris software) provided statistical data on the surface area and volume. The data were analyzed for morphometric scaling and correlation of scaling to predict a proxy for the functional capacity of the digestive system. The specific growth rate (SGR) for each organ was calculated from the volume data using the equation $SGR = (\ln V2 - \ln V1)x(t2 - t1)^{-1}$, where $V2$ is the volume of the organ at time 2 ($t2$), and $V1$ as the initial volume at $t1$.

The 3D models were also used to generate *.pdf* files that permit users to download and view the models in a readily available format (see details in Data S3). In brief, the 3D models in the Imaris software were saved as *.vrl* files, size-reduced in Meshlab (Cignoni et al., 2008), and exported as *.obj* files into Deep Exploration CAD (Right Hemisphere, now SAP Visual Enterprise Author) for scene reconstruction and surface renaming. The files were exported as *.u3d* files, imported into Adobe Acrobat Pro (Adobe System Inc.), and saved as *.pdf* files.

3 | RESULTS

3.1 | Cranial ossification and development of teeth

Based on the sequence and degree of mineralization of the cranial bones in the staging experiment, the following six stages were proposed (Table 1; Figure 1). The stages cover the ballan wrasse from the newly hatched stage until the fish obtain the characteristics of juvenile individuals.

Stage 1. The first bones to ossify in the wrasse larvae were those comprising the *opercular*. The *dorsal* and ventral pharyngeal teeth and *maxillary* were at the stage of ossification. The first teeth formed were the pharyngeal teeth; a few dorsal and ventral pharyngeal teeth were present at stage 1, but no teeth were present on the premaxillary or dentary bones (Figure 2a,b).

Stage 2. The cranium is characterized by jaw ossification. The *premaxillary* and *maxillary* of the upper jaw and the *dentaries* of the lower jaw were now mineralized. The *parasphenoid* in the neurocranium had begun to mineralize. The *dorsal* and *ventral pharyngeal* branchial arches continued the ossification process, and the distinctive

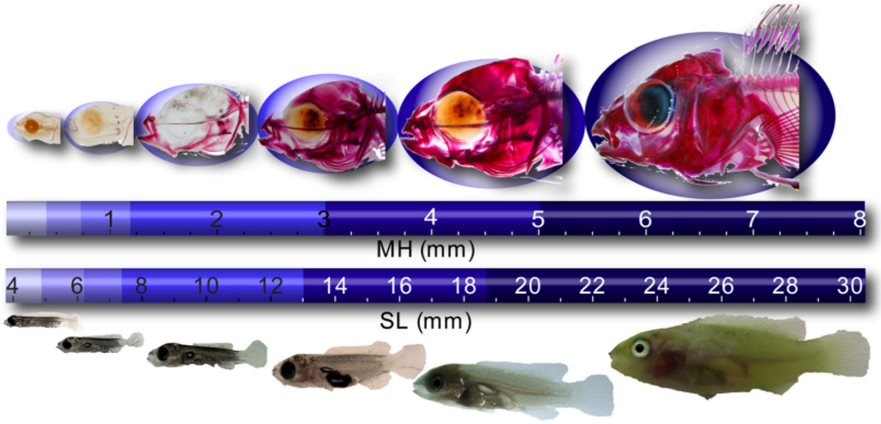

FIGURE 1 Stages of ballan wrasse from 1 to 6. Stages are based on degree of ossification of cranial bones using alizarin red (top) and corresponding myotome height (MH, in mm), standard length (SL, in mm), and outer morphology (bottom)

shapes of these bones were established at the end of stage 2. The pharyngeal teeth were more developed, and in particular, the bone plates to which they are attached were more robust at this stage. The *premaxillary* and *dentaries* were still toothless (Figure 3a,b).

Stage 3. The cranium was well-developed compared to the previous stages, where the *premaxillary*, *maxillary*, and *dentaries* formed their respective distinctive bone shapes. The *ectopterygoid*, *quadrate*, *articular*, and *angular* of the cranium had begun to mineralize. Mineralization was present in the bones of the hyoid arch. Most of the bones of the *opercular* were mineralized and formed their distinctive shapes by the end of this stage. Nine of 17 compartments of the neurocranium had been mineralized and established distinct bone forms. During stage 3, the first teeth appeared on both the upper (*premaxillary*) and lower (*dentary*) jaws (Figure 4a,b).

Stage 4. Stage 4 was characterized by the formation of the distinctive shapes of the compartments comprising the cranium, hyoid arch, opercular, neurocranium, and branchial arches Some bones were still at the initiation of ossification. This stage was best characterized by the "closing" of the neurocranium, by expanding ossification of the *otic* group, particularly the *supraoccipital*, *parietal*, and *frontal* bones. At stage 4, the teeth of the premaxillary and dentary were present and robust in appearance. The pharyngeal teeth had increased significantly in length (Figure 5a,b).

Stage 5. All bone compartments of the head presented mineralization, and some of them were as fully developed as those in adults. All four bones of each *pharyngobranchial*, *epibranchial*, and *ceratobranchial* had formed their distinctive shapes. Three of the four *hypobranchial* were present in this stage. The premaxillary and dentary teeth had grown in length and protruded anteriorly, in the manner characteristic of the adult life stages. The pharyngeal teeth were more numerous, particularly on the ventral side, where the bone had by now taken on a Y shape (Figure 6a,b).

Stage 6. Most bones in the head had attained an adult-like shape. The *premaxillary* and *dentary* have now taken the solid shape characteristic of young adults (Figure 7a,b). The pharyngeal teeth were more numerous and robust, and the ventral tooth-bearing bone plate formed the recognizable shape of the "labrid cross" (Figure 7c,d).

3.2 | Morphological development of the digestive system

Stage 1. The digestive tract was a straight canal located dorsally to the yolk (Figure 2c), and from the start of the esophagus to the anus represented ca. 41% of the SL of the larvae. The esophagus mucosa was a cylindrical and hollow tube with no folding, and no goblet cell was observed (Figure 2d,e). The esophagus was separated from the intestine by an esophageal–intestinal constriction, but at this stage, there was no further distinguished morphology in the remaining tract; there was no bulbus and no differentiation or valve between the midgut and hindgut (Figure 2d). A simple ciliated columnar epithelium (brush border) was present throughout the tract (Figure 2f). The liver was present anteriorly in the abdomen with hepatocytes in a tubular arrangement (Figure 2g), a compact exocrine pancreas was present posterior to the liver, with zymogen granules in the acinar cells (Figure 2h), and the gallbladder was observable between the liver and pancreatic tissue, with the bile duct ending in the lumen of the intestine shortly behind the constriction between the esophagus and the intestine from the ventral side (Figure 2i).

Stage 2. The digestive tract was still a straight tube (gut length to SL ratio of 50%), but one of the obvious changes was a widening of the anterior intestine and almost complete consumption of the yolk (Figure 3c). The digestive tract was compartmentalized into the mucoid esophagus in the rostral region (Figure 3d), the non-mucoid intestine with some proximal enlargement of the diameter (bulbus), and the distal midgut and hindgut separated from each other by the ileorectal valve (Figure 3e,f). The locations of the liver, exocrine pancreas, and gallbladder were similar to those in stage 1 surrounding the anterior bulbus (Figure 3g,h). One primary islet of Langerhans (endocrine pancreas) was observed close to the gallbladder (Figure 3i).

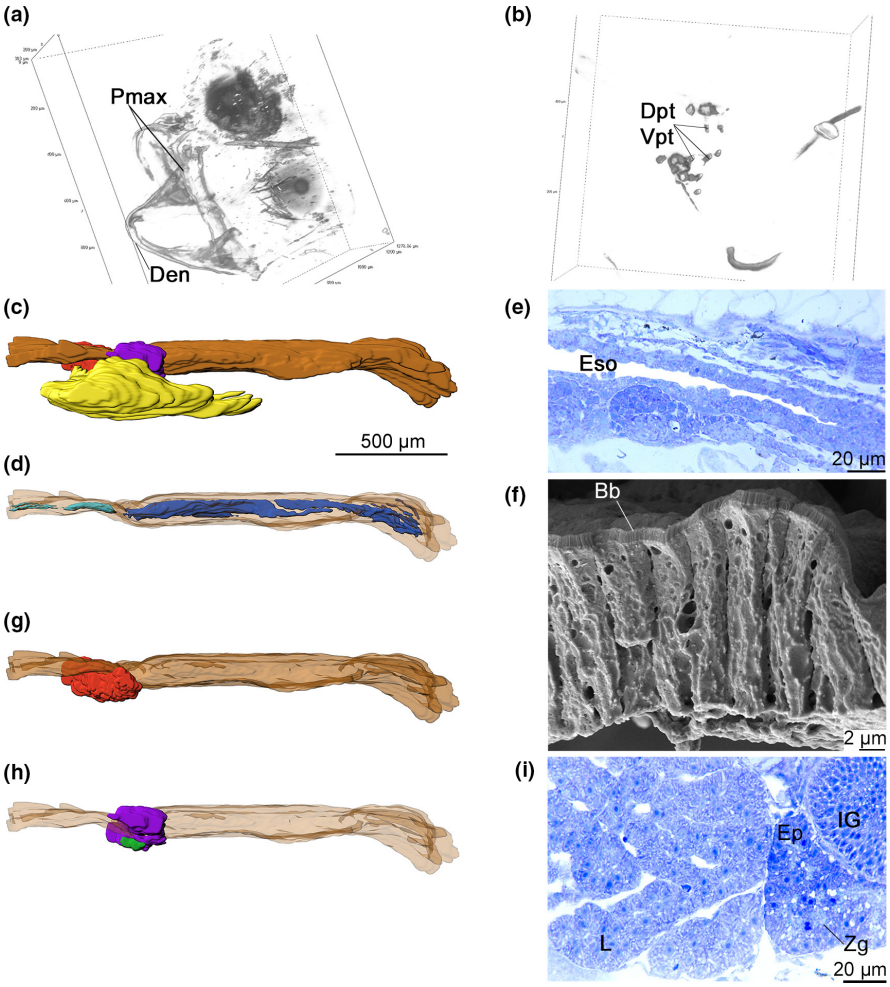

FIGURE 2 Morphology of the digestive system of ballan wrasse stage 1 (a) toothless premaxillary (pmax) and maxillary of the upper jaw and dentary of the lower jaw are the first bones to initiate ossification. (b) Lateral view of dorsal (dpt) and ventral pharyngeal teeth (c) reconstructed 3D model of the left side of the outer morphology of the digestive system from esophagus to anus. (d) Reconstructed 3D model of the left side of the esophageal and intestinal lumen of the digestive tract from esophagus to anus (90% transparency). (e) Non-mucoid and unfolded mucosa of the esophagus (Eso). (f) Scanning electron micrograph showing clear brush border (bb) of the apical end of the enterocytes at stage 1. (g) Reconstructed 3D model of the left side of the liver in relation to the digestive tract (60% transparency). (h) Reconstructed 3D model and partial distribution of the exocrine pancreas and gallbladder with the digestive tract from esophagus to anus (90% transparency). (i) Structure of the liver lobe (L), exocrine pancreas (ep) with zymogen granules (Zg) in acinar cells, and incipient gut (IG). Scale bar in C applies for D, G, and H. light graphs with toluidine blue staining. 3D models—Orange adventitia and serosa of the digestive tract. *Red* liver. *Purple* exocrine pancreas. *Yellow* yolk. *Light blue* lumen esophagus. *Dark blue* lumen intestine. *Green* gallbladder. Bb, brush border; Den, dentary; Dpt, dorsal pharyngeal teeth, Ep, exocrine pancreas, Eso, esophagus; IG; incipient gut, L, liver; Pmax, premaxillary; Vpt, ventral pharyngeal teeth; Zg, zymogen granules

Stage 3. This stage was best characterized by the initial rotation of the gut into one loop (gut length to SL ratio of 57%; Figure 4c) and the pronounced presence of villi in the esophagus and intestine (Figure 4d). The yolk was completely absorbed, and the larvae were thus fully dependent on exogenous feeding for survival. The esophageal mucosa was folded (longitudinal villi from the pharynx until the constriction prior to the intestine; Figure 4e) and showed the formation of a prominent striated external musculature. The anterior intestine (bulbus) did not have a wider diameter than the posterior segment or exhibit any muscular changes (Figure 4f). The folded mucosa of the bulbus consisted of tall longitudinal villi, and their length and number decreased toward the hindgut. The ileorectal valve separating the midgut and hindgut became more distinct compared to that in stage 2. The locations of the liver and gallbladder were similar to those in stages 1 and 2 (Figure 4g). Exocrine pancreatic tissue was more scattered along the intestine than in earlier stages (Figure 4h), with the presence of one primary islet of Langerhans. The pancreatic duct was observed for the first time, terminating in the lumen of the bulbus shortly after the end of the esophagus, along with the common bile duct from the gallbladder, in the form of two separate openings (Figure 4i).

Stage 4. No new tissues or organs were observed at this stage or at any later stages in the study. However, the most obvious distinct trait

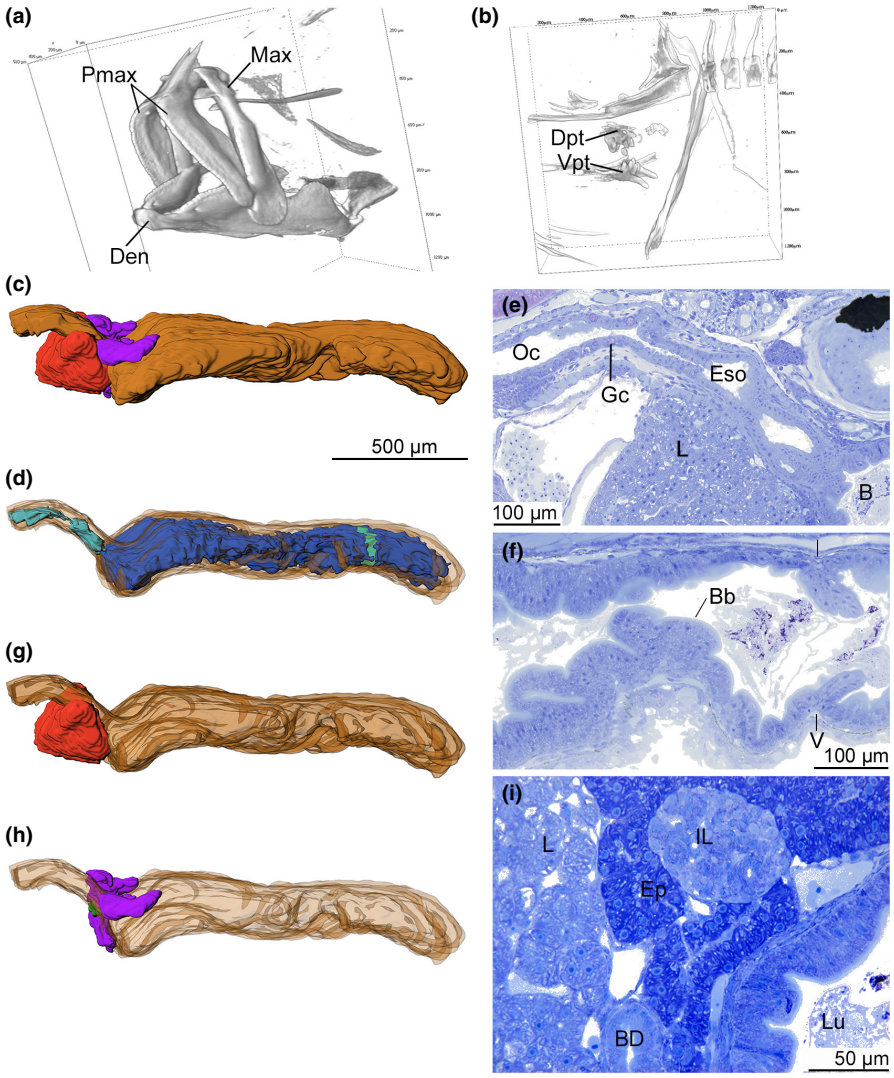

FIGURE 3 Morphology of the digestive system of ballan wrasse stage 2 (a) premaxillary and maxillary (upper jaw) and dentary of the lower jaw are mineralized, no teeth present. (b) Lateral view of dorsal and ventral pharyngeal teeth and maxillary. (c) Reconstructed 3D model of the left side of the outer morphology of the digestive system from esophagus to anus. (d) Reconstructed 3D model of the left side of the esophageal and intestinal lumen of the digestive tract from esophagus to anus (90% transparent serosa). (e) Mucoid esophageal mucosa in the proximal region close to the pharynx (Gc, goblet cells). The esophagus (Eso) ends with a constriction prior to the intestinal bulb (B). (f) Non-mucoid mucosa of the posterior midgut with clear brush border (Bb) and valve (V) prior to hindgut. Mucosa displayed a characteristic leaf-like structure. (g) Reconstructed 3D model of the left side of the liver in relation to the digestive tract (60% transparency) from esophagus to anus. (h) Reconstructed 3D model and partial distribution of the exocrine pancreas and gallbladder with the digestive tract from esophagus to anus (90% transparency). (i) Structure of the liver (L), exocrine pancreas (Ep), and primary islet of Langerhans (IL) located close to the gallbladder and bile duct (BD). Scale bar in C applies for D, G, and H. Light graphs with toluidine blue staining. 3D models—*Orange* adventitia and serosa of the digestive tract. *Red* liver. *Purple* exocrine pancreas. *Light blue* lumen esophagus. *Dark blue* lumen intestine. *Green* gallbladder. B, bulbus; Bb, brush border; BD, bile duct; Den, dentary; Dpt, dorsal pharyngeal teeth; Ep, exocrine pancreas; Eso, esophagus; Gc, goblet cells; IL, Islet of Langerhans; L, liver; Lu, lumen intestine; Max, maxillary, Oc, oral cavity; Pmax, premaxillary; V, valve; Vpt, ventral pharyngeal teeth

at this stage was the lengthening of the intestinal loop and growth of the gut tissue (length equivalent to 58% of SL; Figure 5c). The buccopharyngeal cavity, which in earlier stages was lined with a simple columnar epithelium, had developed a stratified squamous epithelium by stage 4. While the intestinal mucosa was the same as in stage 3, the gut rotated into a Z-shape, while the midgut and hindgut were separated by the ileorectal valve (Figure 5d). The hindgut had a wider diameter than the posterior midgut, with a few goblet cells spread among the epithelia. The liver maintained its shape as a compact organ located anteriorly in the abdominal cavity, ventral to the esophagus, as seen in all the previous stages (Figure 5e). The gallbladder was located on the right side of the digestive tract and between the liver and exocrine pancreas (Figure 5f), terminating in the bulbus next to the pancreatic duct. The exocrine pancreas was scattered along the digestive tract within the abdominal cavity (Figure 5g). One primary islet of Langerhans was identified in the earlier stages.

Stage 5. At stage 5, the intestinal rotation was a single loop (Figure 6c) with a gut length at 66% of the SL. The esophageal mucosa

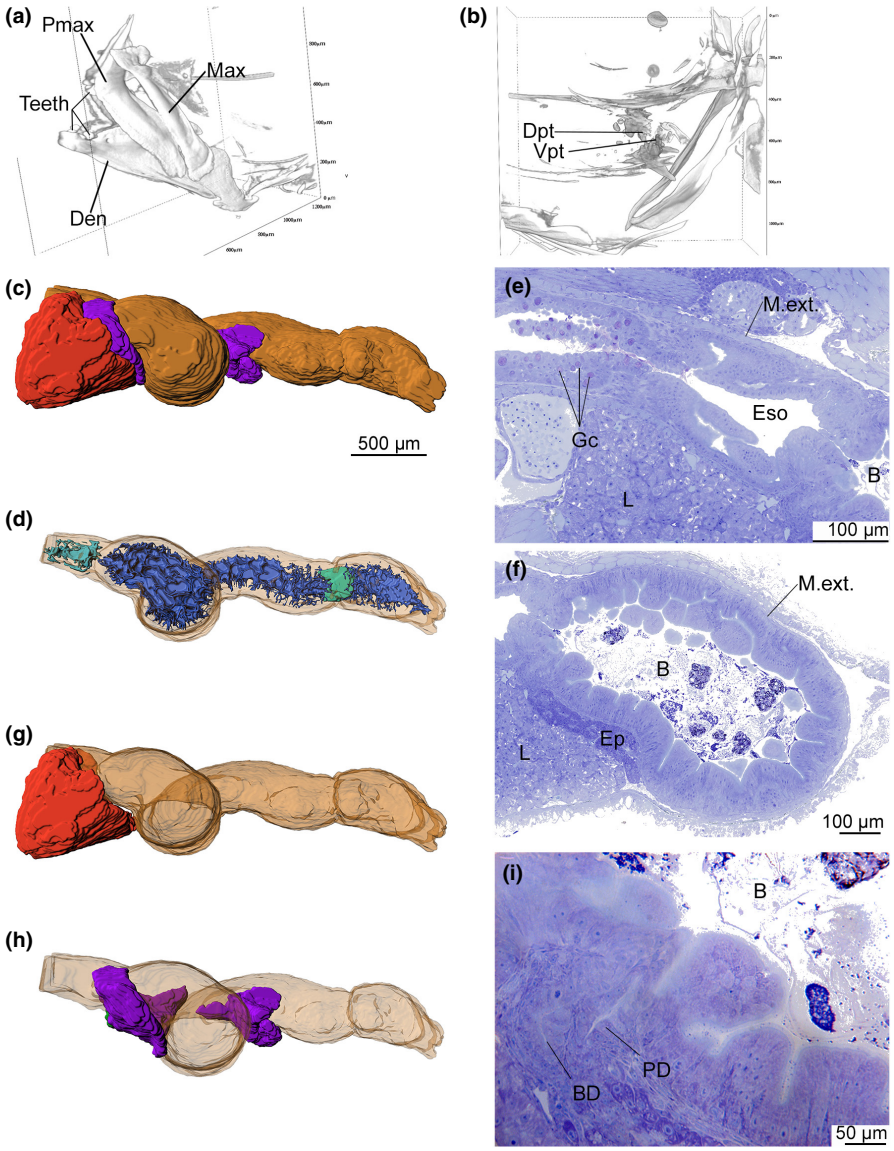

FIGURE 4 External and internal morphological characters of ballan wrasse digestive system at stage 3. (a) Well developed premaxillary, maxillary, and dentary with teeth. (b) Lateral view of dorsal and ventral pharyngeal teeth. (c) Reconstructed 3D model of the left side of the outer morphology of the digestive system from esophagus to anus for stage 3. (d) Reconstructed 3D model of the left side of the esophageal and intestinal lumen of the digestive tract from esophagus to anus (90% transparent serosa). (e) Esophageal mucoid mucosa was surrounded by thick m. externa (M. ext.) where the circular muscle layer was the most prominent layer. The prominent muscle layer was lost when the esophagus enters the intestinal lumen just after the constriction between the esophagus and the bulbus. (f) There were no prominent external muscle layer (M. ext.) surrounding the bulbus. (g) Reconstructed 3D model of the left side of the liver in relation to the digestive tract (60% transparency) from esophagus to anus. (h) Reconstructed 3D model and partial distribution of the exocrine pancreas and gallbladder with the digestive tract from esophagus to anus (serosa at 90% transparency). (i) Entrance of the pancreatic duct (PD) and common bile duct (BD) into the lumen of the bulbus in stage 3 ballan wrasse. The ducts never merged but ended into the lumen as two separate openings. Scale bar in C applies for D, G, and H. Light graphs with toluidine blue staining. 3D models—*Orange* adventitia and serosa of the digestive tract. *Red* liver. *Purple* exocrine pancreas. *Light blue* lumen esophagus. *Dark blue* lumen intestine. *Green* gallbladder. Abbreviations: B, bulbus; BD, bile duct; Den, dentary; Dpt, dorsal pharyngeal teeth; Eso, esophagus; Gc, goblet cells; L, liver; Lu, lumen intestine; Max, maxillary, M. ext., external musculature; PD, pancreatic duct; Pmax, premaxillary; Vpt, ventral pharyngeal teeth

was folded with a high density of goblet cells, particularly at the proximal esophagus (Figure 6d,e). The *muscularis externa* of the esophagus was striated skeletal muscle. Only a few goblet cells were present in the bulbus, but mucoid cells increased posteriorly toward the hindgut, with the highest density in the hindgut along with the smallest villi (Figure 6f). The liver was located posteriorly to the *septum transversum* surrounding the gallbladder, with elongations on the left and ventral sides of the midgut all the way to the hindgut, unlike in

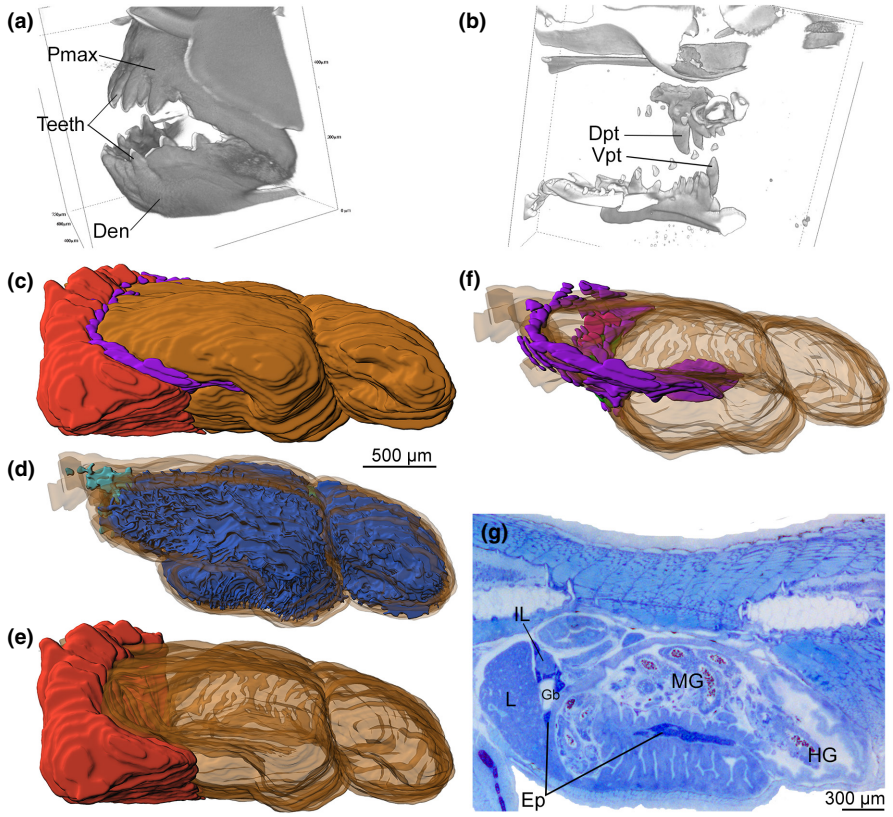

FIGURE 5 External and internal morphological characters of ballan wrasse larvae at stage 4. (a) Well developed premaxillary, maxillary, and dentary with robust teeth. (b) Lateral view of dorsal and ventral pharyngeal teeth. (c) Reconstructed 3D model of the left side of the outer morphology of the digestive system from esophagus to anus for stage 4. (d) Reconstructed 3D model of the left side of the esophageal and intestinal lumen of the digestive tract from esophagus to anus (90% transparent serosa). (e) Reconstructed 3D model of the left side of the liver in relation to the digestive tract (60% transparency) from esophagus to anus. (f) Reconstructed 3D model and partial distribution of the exocrine pancreas and gallbladder with the digestive tract from esophagus to anus (serosa at 90% transparency). (g) Mid-longitudinal section of the digestive system of stage 4 ballan wrasse larva—intestinal rotation of midgut (MG). Scale bar in C applies for D, E, and F. Light graphs with toluidine blue staining. 3D models—*Orange* adventitia and serosa of the digestive tract. *Red* liver. *Purple* exocrine pancreas. *Light blue* lumen esophagus. *Dark blue* lumen intestine. *Green* gallbladder. Den, dentary; Dpt, dorsal pharyngeal teeth; Ep, exocrine pancreas; GB, gallbladder; HG, hindgut; IL, Islet of Langerhans; L, liver; MG, midgut; Pmax, premaxillary; Vpt, ventral pharyngeal teeth

the previous stages (Figure 6g). In addition to the elongations, the left and right sides of the liver were connected both dorsally and ventrally to the esophagus, whereas in earlier stages, this was limited to only the ventral side of the esophagus. The exocrine pancreas was scattered within the abdominal cavity and near the larger blood vessels within the liver (Figure 6h). This was the first stage when several islets of Langerhans were observed; one primary islet (the largest, in the same region as in stages 2–4), located proximally to the gallbladder, was surrounded by several smaller islets located close to the large primary islet (Figure 6i). The bile duct and pancreatic duct entered an anterior bulbus.

Stage 6. The digestive system in stage 6 is fully developed. As in stage 5, the presence of a bulbus of the proximal intestine and Z-shaped rotation of the gut persisted, while the mucosal folding of the intestine became progressively shorter from the bulbus toward the anus, while the gut length increased to 69% of SL. The bulbus had a wider diameter and narrowed prior to the rotation of the digestive tract, as seen in earlier stages (Figure 8a,b), but no prominent *muscularis externa* was observed around or after the bulbus, and no valve after the bulbus, indicating a non-functional pseudogaster (Figure 8c). The epithelium of the intestine had matured compared to 4 dph (stage 1), with a taller columnar cell height of 22.12 ± 2.22 µm and a diameter of 3.19 ± 0.64 µm with microvilli (height 0.72 ± 0.16 µm) throughout the intestine (Figure 8d). The liver maintained a compact shape located anteriorly in the abdomen until after metamorphosis (stage 5) when it became elongated ventrally of the rotated midgut all the way to the hindgut (Figure 8e). Low-fat accumulation in hepatocytes with very small changes during ontogeny indicated a low-fat liver in ballan wrasse (Figure 8f). Exocrine pancreatic tissue was scattered within the abdominal cavity and regularly present within the liver around the larger blood vessels, as seen in stage 5 (Figure 8f,g). Connective tissue within the exocrine pancreas included large populations of immune cells, especially eosinophilic granular cells (Figure 8h). A few eosinophilic granular cells were also present in the submucosa and serosa of the digestive tract, but not as prominently as in the exocrine pancreas. Although the exocrine pancreas was scattered, only one pancreatic duct was observed, terminating next to the common bile duct in the bulbus.

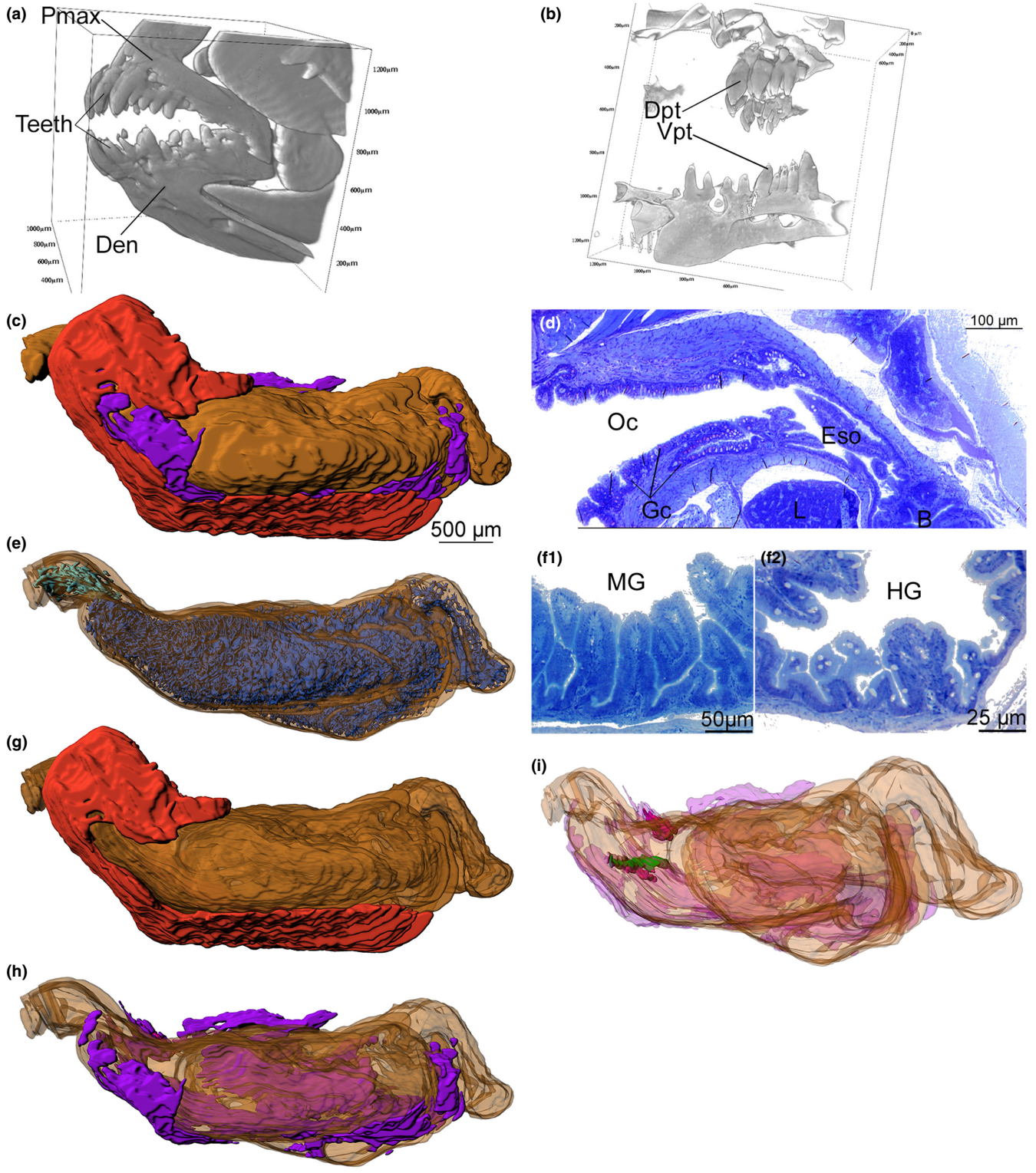

3.3 | Growth and morphometric scaling of the digestive system

The surface areas and volumes of all organs were retrieved from Imaris Measurement Pro. The outer surface area (adventitia and serosa) of the digestive tract increased 59 times from stage 1 to stage 6 (0.99–58.40 mm^2), while the esophageal and intestinal lumen increased 184 and 464 times, respectively, not including microvilli (Table 2). Surface area of the esophageal mucosa grew gradually from 0.02 to 3.64 mm^2 from stages 1 to 6, while the intestinal mucosa increased from 0.23 to 106.75 mm^2. The surface area of the liver for stages 1–5 increased from 0.20 to 38.81 mm^2, falling to 30.67 mm^2 at stage 6. Exocrine pancreatic tissue grew from 0.15 to 34.47 mm^2 from stages 1 to 6, while the endocrine pancreas increased between stages 2 and 6 from 0.02 to 0.65 mm^2.

FIGURE 6 External and internal morphological characters of ballan wrasse larvae at stage 5. (a) Well developed premaxillary, maxillary, and dentary with anterior protruded teeth. (b) Lateral view of dorsal and ventral pharyngeal teeth. Numerous ventral pharyngeal teeth. (c) Reconstructed 3D model of the left side of the outer morphology of the digestive system from esophagus to anus. The massive liver as a compact organ covering the ventral surface of the digestive tract and the exocrine pancreas was spread out to fill the empty spaces between the liver and the digestive tract. (d) Mid-longitudinal section of the mucoid mucosa of distal oral cavity, pharynx, and proximal esophagus. (e) Reconstructed 3D model of the left side of the esophageal and intestinal lumen of the digestive tract from esophagus to anus (90% transparent serosa). (f1) Low density of goblet cells in midgut mucosa. (f2) higher density of goblet cells in hindgut mucosa. (g) Reconstructed 3D model of the left side of the liver in relation to the digestive tract (60% transparency) from esophagus to anus. (h) Reconstructed 3D model and partial distribution of the exocrine pancreas and gallbladder with the digestive tract from esophagus to anus (serosa at 90% transparency). (e) Several islets of Langerhans (dark pink) were observed in stage 5. One larger primary islet is located on the right side of the digestive tract and several smaller islets nearby. Scale bar in C applies for E, G, H, and I. light graphs with toluidine blue staining. 3D models—*Orange* adventitia and serosa of the digestive tract. *Red* liver. *Purple* exocrine pancreas. *Light blue* lumen esophagus. *Dark blue* lumen intestine. *Green* gallbladder. B, bulbus; Den, dentary; Dpt, dorsal pharyngeal teeth; Eso, esophagus; GC, goblet cells, HG, hindgut; L, liver; Max, maxillary, MG, midgut; OC, oral cavity; Pmax, premaxillary; Vpt, ventral pharyngeal teeth

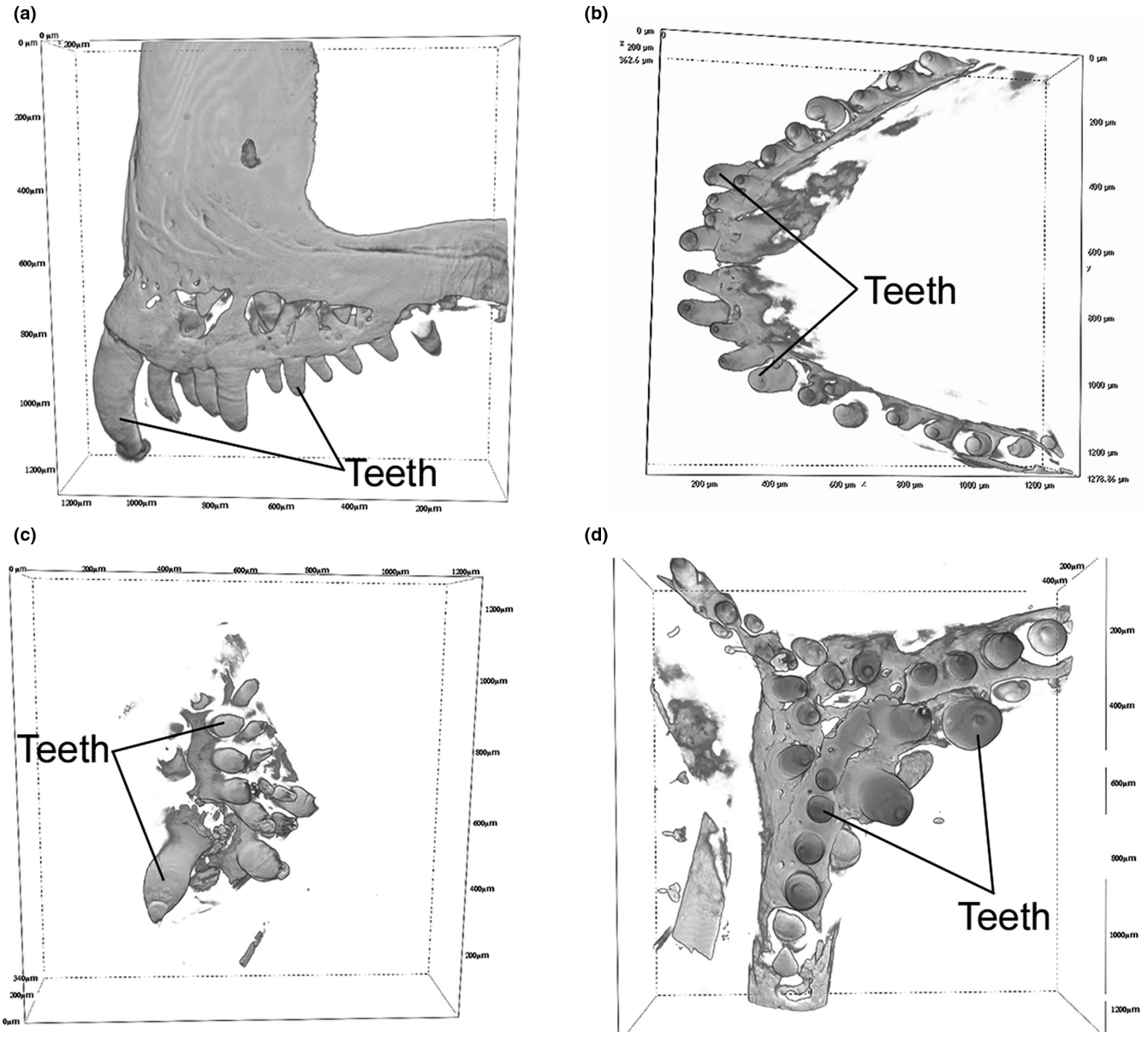

FIGURE 7 Teeth in stage 6 ballan wrasse. (a) Lateral view of teeth up the upper jaw. (b) Dorsal view of teeth of lower jaw. (c) Ventral view of dorsal pharyngeal teeth. (d) Ventral pharyngeal teeth on a ventral, Y-shaped teeth bearing bone plate, forming the "labrid cross"

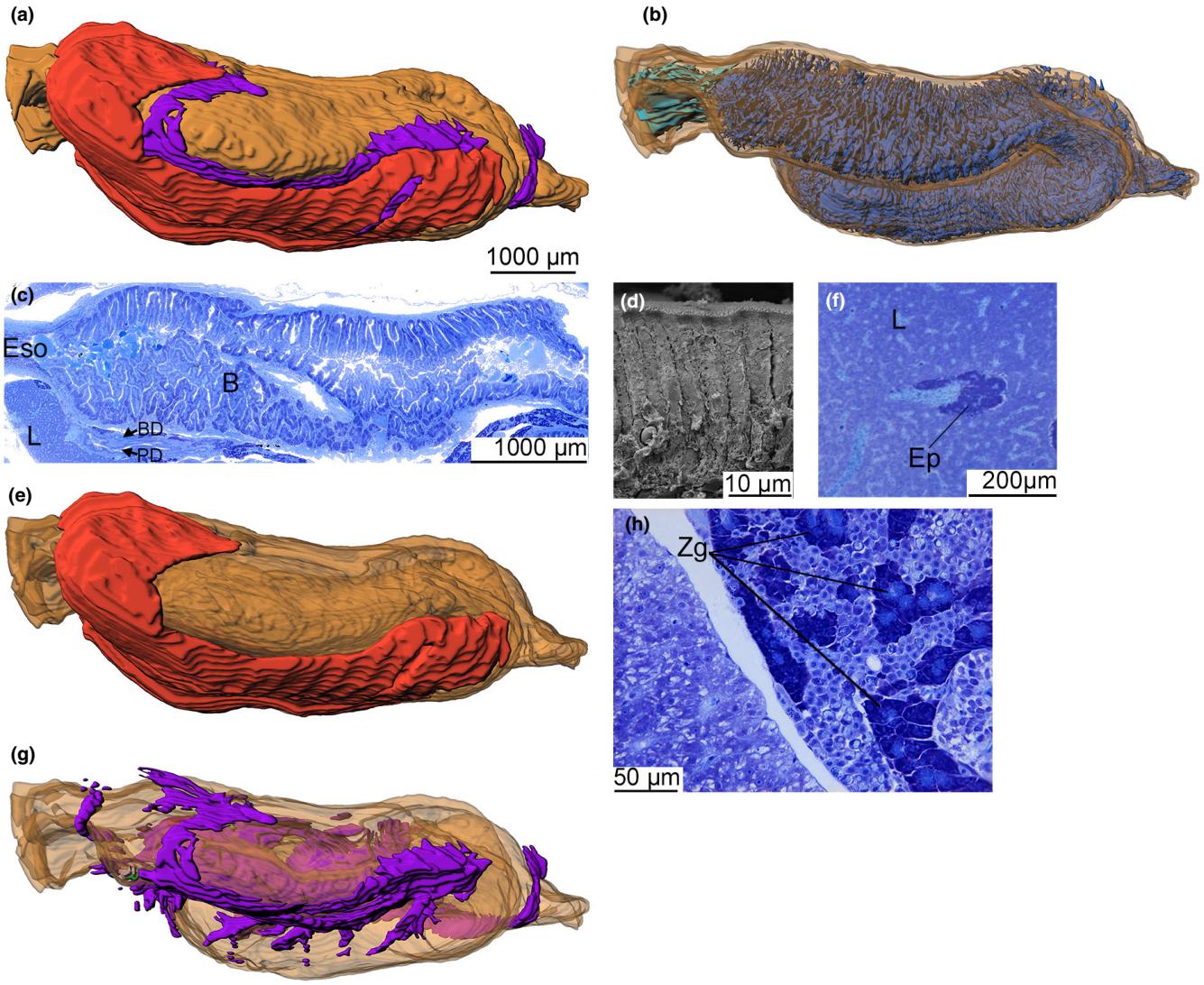

FIGURE 8 External and internal morphological characters of ballan wrasse digestive system at stage 6. (a) Reconstructed 3D model of the left side of the outer morphology of the digestive system from esophagus to anus. (b) Reconstructed 3D model of the left side of the esophageal and intestinal lumen of the digestive tract from esophagus to anus (90% transparent serosa). (c) Mid-longitudinal section of the esophagus and bulbus. Prominent external muscle layer diminishes in the bulbus region. (d) Scanning electron micrographs of the tall, hexagonal-shaped enterocytes covered with brush border in the apical end. (e) Reconstructed 3D model of the left side of the liver in relation to the digestive tract (60% transparency) from esophagus to anus. (f) Exocrine pancreatic tissue was scattered within the abdominal cavity and regularly present within the liver around the larger blood vessels. (g) Reconstructed 3D model and partial distribution of the exocrine pancreas and gallbladder with the digestive tract from esophagus to anus (serosa at 90% transparency). (h) Tubular arrangement of zymogen granules (Zg) of the exocrine pancreatic acinar cells. The connective tissue surrounding acinar cells was infiltrated by immune cells, particularly eosinophilic granular cells. Scale bar in (a) applies for (b), (e) and (g). Light graphs with toluidine blue staining. 3D models—*Orange* adventitia and serosa of the digestive tract. *Red* liver. *Purple* exocrine pancreas. *Light blue* lumen esophagus. *Dark blue* lumen intestine. *Green* gallbladder. B, bulbus; BD; bile duct, ep, exocrine pancreas; Eso, esophagus; L, liver; PD, pancreatic duct; Zg, zymogen granules

The volumes (as an indicator of tissue mass) from stages 1 to 6 grew from 0.01 to 8.69 mm^3 for the outer surface of the digestive tract, 0.00005–0.06 mm^3 for the esophageal lumen, and 0.0006–3.76 mm^3 for the intestinal lumen (microvilli not included; Table 3). The volume of gut tissue, measured as the volume of esophageal and intestinal lumen subtracted from the volume of the digestive tract, rose from 0.01 mm^3 at stage 1 to 4.87 mm^3 at stage 6. The volume of the liver developed in a manner similar to that of the surface area, increasing from 0.001 to 3.10 mm^3 from stages 1 to 5 and decreasing to 2.09 mm^3 by stage 6. Exocrine pancreas volume expanded from 0.001 to 0.92 mm^3 for stages 1–6, and the endocrine pancreas from 0.0001 to 0.01 mm^3 from stage 2 to 6.

The relative volumes (percentage of the different examined tissues and organs at a stage) were calculated from the combined volumes of gut tissue, liver, exocrine, and endocrine pancreas (Table 4). At the onset of feeding, the gut tissue displayed the largest relative volume (78.9%), while the liver and exocrine pancreas were 13.5% and 7.6%, respectively. After metamorphosis, the gut tissue remained the largest organ (61.6%), followed by the liver (26.5%), and exocrine pancreas (11.7%), while the

TABLE 2 Surface areas (mm^2) of external surface of the digestive tract (adventitia and serosa), esophageal lumen, intestinal lumen, liver, exocrine and endocrine pancreatic tissue from stage 1 until stage 6 in ballan wrasse

Stage	Adventitia and serosa (mm^2)	Esophageal mucosa (mm^2)	Intestinal mucosa (mm^2)	Liver (mm^2)	Exocrine pancreas (mm^2)	Endocrine pancreas (mm^2)
1	0.99	0.02	0.23	0.20	0.15	
2	3.71	0.23	2.52	0.66	0.42	0.025
3	3.88	0.15	3.10	1.37	1.18	0.04
4	12.94	0.43	13.47	5.18	2.29	0.13
5	56.30	3.26	102.86	38.81	30.49	0.88
6	58.40	3.64	106.75	30.67	34.47	0.65

TABLE 3 Volumes (mm^3) of gut tissue, liver, and exocrine and endocrine pancreatic tissue from stages 1 to 6. Gut tissue volumes were calculated as (volume of the outer surface of the digestive tract) minus (sum of volumes of esophageal and intestinal lumens)

Stage	Gut tissue (mm^3)	Liver (mm^3)	Exocrine pancreas (mm^3)	Endocrine pancreas (mm^3)
1	0.01	0.001	0.001	
2	0.06	0.01	0.004	0.0001
3	0.16	0.05	0.01	0.0002
4	0.33	0.11	0.02	0.0007
5	5.70	3.10	0.79	0.01
6	4.87	2.09	0.92	0.01

TABLE 4 Relative volumes (%) of the gut tissue, liver, and pancreatic tissues for stages 1–6. The relative volumes were calculated by dividing the volume of each organ/tissue by the combined volumes of gut tissue, liver, exocrine and endocrine pancreas at each stage

Stage	Gut tissue (%)	Liver (%)	Exocrine pancreas (%)	Endocrine pancreas (%)
1	78.9	13.5	7.6	
2	76.8	18.0	5.0	0.2
3	71.7	21.6	6.6	0.1
4	71.0	24.1	4.7	0.2
5	59.3	32.3	8.2	0.2
6	61.6	26.5	11.7	0.2

endocrine pancreas remained stable at 0.1%–0.2% throughout development.

The SGR was calculated for each organ between each consecutive stage (1–2, 2–3, 3–4, 4–5, 5–6) and from stages 1 to 6, given as percentage increase in volume per day (Table 5). All organs displayed strong growth between stages 1 and 2 and gradually declined toward stage 6. From stages 1 to 6, gut tissue, liver, and exocrine pancreas displayed a growth of $6.72 \pm 0.39\%$ day^{-1}, while the endocrine pancreas displayed a strong SGR of 16.93% day^{-1} from stages 1 to 6.

TABLE 5 Specific growth rate (SGR; % day^{-1}) of key digestive organs in ballan wrasse calculated from volume data between each stage (1–2, 2–3, 3–4, 4–5, 5–6) and from stages 1 to 6

Stages	1–2	2–3	3–4	4–5	5–6	1–6
Gut tissue	29.20	11.64	6.31	6.75	−0.51	6.18
Liver	34.46	14.80	7.35	7.88	−1.27	7.12
Exocrine pancreas	22.59	15.96	3.41	8.50	0.51	6.87
Endocrine pancreas	201.61	4.93	9.64	7.71	−0.63	16.93

3.4 | Body size, age, and correlation to stages

The correlations between SL, MH, age (dph), and developmental stage were investigated (Figure 9). The curves showing the correlation between SL and MH at different stages have different slopes. Stages 1 and 2 had the same ratio of MH to SL, whereas the MH:SL ratio increased in the four older stages (Figure 9e,f). Age, SL, and MH were strongly correlated with stages, with R^2 values of 0.980, 0.960, and 0.995, respectively.

4 | DISCUSSION

Nearly all scientific work describing the digestive apparatus of fish starts with the esophagus. However, in labroid fish, the processing and mechanical breakdown of food begins, arguably, with the pharyngal teeth. The adult ballan wrasse has both oral and pharyngeal teeth, similar to cichlids, but unlike cyprinids that only possess pharyngeal teeth (Van der Heyden et al., 2005). The ontogeny of teeth in wrasse change according to the kinematics of feeding and is related to their feeding biology and dietary niche (St John et al., 2020). At the start of feeding (stage 1), the larvae have only sharp pharyngeal teeth pointing in the caudal direction. This is the perfect apparatus to ensure that the captured zooplankton do not escape, but instead, end up in the intestine. A similar order of teeth development is found in other non-related fish species, such as Atlantic cod (Sæle et al., 2017) and Mexican cavefish *Astyanax mexicanus* (Atukorala & Franz-Odendaal, 2014). At stage 4, the dentary and pre-maxillary teeth are present. The shape and anteriorly protruding orientation of the teeth show that they are optimized to bite prey on substrates (Clifton &

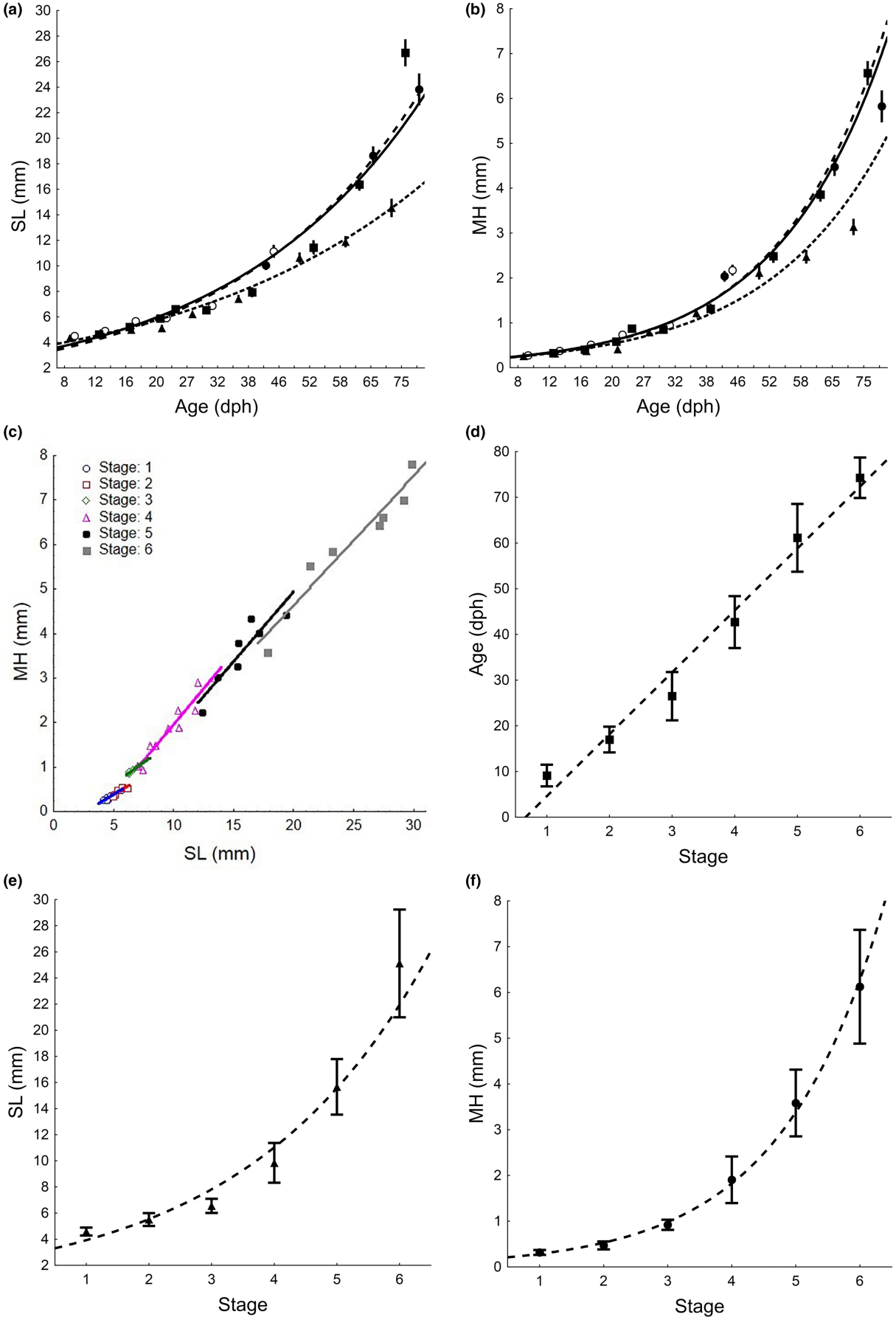
(a)
SL (mm)
Age (dph)
(b)
MH (mm)
Age (dph)
(c)
Stage: 1
Stage: 2
Stage: 3
Stage: 4
Stage: 5
Stage: 6
MH (mm)
SL (mm)
(d)
Age (dph)
Stage
(e)
SL (mm)
Stage
(f)
MH (mm)
Stage

FIGURE 9 Correlations between SL or MH and age or stage. (a). SL and age; tank 1 (◌) and subsequently 6 (●): SL (mm) = 3.4495*exp (0.0781*x). Tank 7 (■): SL (mm) = 3.2611*exp (0.0818*x). Tank 8 (▲): SL (mm) = 3.7644*exp (0.0604*x). (b) MH and age; tank 1 (◌) and subsequently 6 (●): MH (mm) = 0.2208*exp (0.1431*x). Tank 7 (■): MH (mm) = 0.2101*exp (0.1471*x). Tank 8 (▲): MH (mm) = 0.2153*exp (0.1297*x). (c) MH and SL; stage 1: $Y = -0.4361 + 0.1643^*x$; $p = 0.00003$; $r^2 = 0.9005$. Stage 2: $Y = -0.3897 + 0.1563^*x$; $p = 0.0200$; $r^2 = 0.7785$ stage 3: $Y = -0.3713 + 0.1971^*x$; $p = 0.0261$; $r^2 = 0.9485$. Stage 4: $Y = -1.2814 + 0.3236^*x$; $p = 0.00001$; $r^2 = 0.9339$. Stage 5: $Y = -1.3356 + 0.3139^*x$; $p = 0.0037$; $r^2 = 0.8404$. Stage 6: $Y = -1.1707 + 0.2905^*x$; $p = 0.0005$; $r^2 = 0.9293$. (d) Age and stage; $y = 13.557x - 8.9935$. $R^2 = 0.980$ slightly better than exponential: $Y = 6.9237e^{0.4231x}$. $R^2 = 0.976$. (e) SL at six stages; $y = 2.7837e^{0.3442x}$. $R^2 = 0.960$. (f) MH at six stages; $y = 0.1541e^{0.6177x}$. $R^2 = 0.995$. MH, myotome height; SL, standard length

Motta, 1998). It is therefore reasonable to argue that from stage 3 to 4, the ballan wrasse larvae change from feeding uniquely on pelagic zooplankton to being able to feed on invertebrates living on kelp and rocks (Carr & Motta, 2020). At the same time, the pharyngal teeth become blunter, eventually taking a more molar form in adults.

The overall ontogeny of the digestive system in ballan wrasse larvae and juveniles observed in this study compares well with previous studies of the digestive system in ballan wrasse (Dunaevskaya, 2012; Gagnat et al., 2016; Piccinetti et al., 2017) and other marine teleosts (Gisbert et al., 2004, Falk-Petersen, 2005, Sala et al., 2005, Kamisaka & Rønnestad, 2011, Gomes et al., 2014). The esophagus represents the transition from the mouth to the intestine and is derived from the anterior foregut (Govoni et al., 1986). At first feeding (stage 1), the esophagus had an unfolded, nonmucoid cylindrical shape and terminated in a constriction before the incipient intestine, which along with the pharyngeal teeth prevent potential escape of zooplankton. In the juvenile ballan wrasse (stage 6), the esophagus consisted of a longitudinally folded mucoid simple cuboidal epithelium and striated *muscularis externa* from the esophagus until the constriction prior to the bulbus. The time of appearance of goblet cells is species-specific, but is usually prior to or at the onset of exogenous feeding and is thus similar to other species (Bisbal & Bengtson, 1995; Yúfera & Darías, 2007; Zambonino Infante et al., 2008), though in some cases it occurs after the onset of exogenous feeding (Gisbert et al., 2004; Micale et al., 2006). Mucus-producing goblet cells play an important role because fish lack salivary glands: they help lubricate ingested food particles and avoid abrasion from ingested feed, particularly including small crustaceans with exoskeletons and sometimes sharp spines and antennae. The mucus also acts as a barrier against bacterial infections, and it has been suggested that its acidity assists in pregastric digestion in altricial larvae (Baglole, 1997; Gisbert et al., 2004; Yúfera & Darías, 2007). The longitudinal folding of the esophagus, particularly between stages 4 and 6, increases the surface area and provides the capacity to increase the diameter, enabling the passage of larger food items. Together with efficient mucus production, this permits the ballan wrasse to adapt to a new feeding mode with different and larger prey (Yúfera & Darías, 2007).

Ballan wrasse larvae and juveniles have a short digestive tract. At the onset of exogenous feeding (stage 1), the relative length was measured to be 41% of the SL, which correlates with the reported short gut length (often less than 50% of the body length) at the onset of feeding in other marine fish larvae (Rønnestad et al., 2013). The relative length of the digestive tract increased to 57% of SL in stage 3, and then gradually increased to 69% of the SL in juveniles (stage 6), supporting a carnivorous diet despite the short intestine (Dipper et al., 1977; Figueiredo et al., 2005). The intestine occupied the largest percentage volume (60%–80%) of the digestive system, developing—from stage 2 onwards—from an incipient gut into a segmented gut, divided into a proximal midgut with a bulbus of increased lumen diameter, a middle and distal midgut, and finally—separated by a valve—the hindgut. Elongation of the digestive tract—along with differentiation of the segments, cranial ossification, and the appearance of teeth—implies the need for a rigid skull and teeth when ballan wrasse, in its natural habitat, transitions into feeding on invertebrates living on kelp and rocks (Carr & Motta, 2020).

Although a functional bulbus was not observed, the rotation of the gut might reduce the rate of digesta passage and increase the residence time of the digested food to enhance digestive and absorptive efficiency. If there were no food retention and no valves, the gut transit would be faster, and food would pass straight through the digestive tract. The ileorectal valve serves as a one-way valve into the hindgut compartment. In ballan wrasse, an increased muscle bundle around the valve only became prominent in stage 6 (102 dph) juveniles. Previous studies have shown that the bulbus does not function as a storage compartment for food, as demonstrated by the fast passage rate to the next segment, and that ballan wrasse has a faster gut evacuation than do other species (Le et al., 2021; Le, Shao, et al., 2019). However, there must be some delay in the food passage, wherein patterns of peristaltic contractions of the intestinal wall, and operation of the ileorectal valve, can together play a role in increasing the residence time, thereby contributing to the digestion and absorption of nutrients. Cholecystokinin (CCK), a digestive hormone, has been demonstrated to play a key role in regulating the motility and food passage rates in the Ballan wrasse intestine (Le, Lie, et al., 2019). Moreover, the proximal, middle, and distal midgut seem to have a similar absorptive function (Lie et al., 2018).

The formation of villi appeared between stages 2 and 3. The thickening and increased folding of the intestinal mucosa indicate the importance of increasing the surface area for absorption in the first period after hatching, wherein the larvae transfer from endogenous to exogenous feeding to maximize nutrient absorption from the food, together with enhanced activity of membrane enzymes in the brush border (Zambonino Infante & Cahu, 2001). The increased processing performed by the digestive tract is likely to require an enhanced capacity to process the absorbed nutrients (Pelletier et al., 1994). Since the liver has a key role in managing the post-absorptive flow of incoming nutrients from the digestive tract, the liver seems to respond to the growth requirement with a strong specific growth rate of liver tissue in ballan wrasse.

The liver is the major metabolic organ and an important storage organ for energy, and it also produces bile, which is important for lipid digestion. The liver was present from stage 1, and between stages 4 and 5 (29 and 71 dph), the liver developed from a compact form to an elongated form located anterior and ventral to the midgut and all the way to the hindgut. There were low levels of fat deposit in the hepatocytes. Liver size and fat deposition have been observed to be temperature dependent (Cavrois-Rogacki et al., 2019). The liver size may increase as a result of hypertrophy and hyperplasia, as seen in Atlantic cod larvae (Wold, 2007). Increased liver size allows for higher production of bile acids by hepatocytes. The bile is secreted and stored in the gallbladder. The gallbladder in the ballan wrasse was permanently located on the right side of the digestive tract from the early stages, and the common bile duct terminated in the lumen of the bulbus on the ventral side, adjacent to the pancreatic duct. This location permits the bile and pancreatic enzymes to be secreted into the anterior part of the midgut, in the bulbus, just after the feed enters the gut, with the result that chemical digestion can be initiated immediately.

The exocrine pancreas was present—as a compact organ posterior to the liver—from the first feeding (stages 1–2). During development, the pancreas became elongated and scattered within the abdomen between the liver and the digestive tract, in addition to the exocrine pancreas surrounding larger blood vessels within the liver from stage 5 onwards, also referred to as the hepatopancreas. The elongated parts of the exocrine pancreas around the digestive tract, especially in the juvenile ballan wrasse, may help to minimize the distance for transporting signaling molecules—including the hormones CCK and leptin (Le, Lie, et al., 2019)—between the two tissues for the release of digestive enzymes stored in the zymogen granules.

Prior to the formation of a functional stomach in fish larvae, the pancreatic tissue is found together with or in-between the liver tissue, this is sometimes referred to as hepatopancreas as in catfish *Siluriformes* (Mumford et al., 2007) and red-banded seabream *Pagrus auriga* (Sánchez-Amaya et al., 2007). However, hepatopancreas in teleost fish still has dedicated pancreatic tissue and hepatocytes and must not be confused with true hepatopancreas in invertebrates. As the stomach and pyloric caeca form in these species, the pancreatic tissue form in-between the caeca and the liver has the appearance as a defined organ (Mumford et al., 2007; Sánchez-Amaya et al., 2007). In agastric species the pancreatic tissue form along the intestine after the metamorphosis (Al-Hussaini, 1949; Gagnat et al., 2016; Kjørsvik et al., 2014). Gagnat et al. (2016) proposed that the development of the hepatopancreas occurred concurrently with metamorphosis in ballan wrasse. Zymogen granules within the acinar cells of the exocrine pancreas were observed in stage 1 and appear just before or soon after the start of exogenous feeding, indicating a functional pancreas and an actively feeding fish (Mitra et al., 2015; Zambonino Infante & Cahu, 2001).

Trypsin secreted from zymogen granules is considered the key digestive enzyme in fish (Zambonino Infante & Cahu, 1994). In ballan wrasse larvae, trypsin mRNA expression is age-related; it is very low in the yolk-sac stage, peaks around weaning (24–27 dph) and decreases again in older larvae (Hansen et al., 2013). A similar trend of trypsin expression peaking around weaning and declining after metamorphosis was observed in the larval Atlantic cod, presumably because of the formation of gastric glands (Kortner et al., 2011). As ballan wrasse lack gastric glands and peptic digestion (Lie et al., 2018), this could indicate larger and more important roles of other alkaline proteolytic enzymes (i.e., chymotrypsin and elastase) in digestion, and a lower synthesis of trypsin (Hansen et al., 2013). Hansen et al. (2013) suggested that increased lipid and carbohydrate digestion could be a cause for this decrease, where the endocrine regulation of blood glucose is important for homeostasis. In the present study, one islet of Langerhans was observed at stage 2, developing in later stages to one primary islet with smaller nearby islets, and displaying a growth rate about twice that of other digestive organs. This may support an altered postabsorptive hormonal and metabolic state in ballan wrasse during the ontogeny of the digestive system from larval to juvenile stages, and to deal with the associated gradual changes in diet.

In terms of absolute morphological scaling, the digestive organs generally increased in both volume and surface area as the larvae grew. For the gut tissue, the relative growth of volume and surface area showed a peak in the earliest stages (1–2), followed by a slower increase (stage 2–4), a new peak between stages 4 and 5, and then an even lower growth rate in juvenile ballan wrasse (stages 5–6). A possible strategy for growth of digestive organs was suggested by the Segner et al. (1994) research on turbot *Scophthalmus maximus*, which proposed that the fish first invest in elongating the digestive tract to increase the gut passage rate for digestion, and then in a second phase increase the mucosal surface area to strengthen the absorptive efficiency. Increasing the mucosal surface area is also a priority for ballan wrasse larvae. However, turbot develops a stomach during metamorphosis and acquire a longer gut (114% of SL at post-metamorphosis; Segner et al., 1994), while ballan wrasse have a shorter gut and no stomach. Le et al. (2019) showed that CCK reduced the passage of digesta and suggested that this was an adaptation to keep digesta in the intestine for better digestion to compensate for the missing stomach. The ballan wrasse seemed to invest variously in gut length, surface area, and tissue mass (volume) in the earliest stages (1–2), while the exocrine pancreas, liver, and endocrine pancreas showed a rapid volume increase in the later stages (stages 4–5). As juveniles, there was a decline in liver volume, while the exocrine pancreas increased in volume between stages 5 and 6. Gagnat et al. (2016) hypothesized that the morphometric decline of the liver and a minor increase in the exocrine pancreas could be explained by the formation of the hepatopancreas.

Numerous eosinophilic granular cells (eosinophils) were observed within the connective tissue between the exocrine pancreas, intestinal *submucosa* and between the intestinal *serosa* of juvenile ballan wrasse (stage 6, 102 dph); similar infiltration of immune cells are observed in previous non-pathological histological characteristics of ballan wrasse (Helland et al., 2014; Le et al., 2019; Zhou et al., 2021). The real function of these cells is unknown, but it has been suggested that they are related to a defense mechanism (Mumford et al., 2007). Interestingly, it has been shown that the

ballan wrasse intestine has an extraordinarily elevated level of immune activity (Bilal et al., 2019; Zhou et al., 2021), supporting the possibility of a defense mechanism in the absence of a stomach.

From the larval to juvenile stage (stages 1–6), the relative volume of the gut tissue declined (from 79% at stage 1 to 61% at stage 6), while that of the exocrine pancreas increased from 7% to 11% and—together with the liver—increased in total relative volume from 21% to 38%. An opposite pattern with decreasing relative volume of the liver and pancreas is observed when the proximal midgut develops from a bulbus to a functional stomach, as seen in Atlantic cod (Kamisaka & Rønnestad, 2011) and common dentex (Sala et al., 2005); in ballan wrasse, however, secretions from the exocrine pancreas play a larger role in digestion when the stomach is lost (Lie et al., 2018). The growth of the pancreas and liver in ballan wrasse likely emphasize the importance of their roles in agastric fish, as neuronal and hormonal regulation of digestion and appetite are crucial for survival. The growth of the digestive system from stages 5 to 6 was very low, as was the presence of adult-like bones in the skull and solid dentary apparatus, suggesting an allocation of energy toward other aspects including the growth of skeletal muscles.

5 | CONCLUSION

In this study, we established six developmental stages for ballan wrasse from the first feeding until the juvenile stage, supported by cranial ossification, maturation of the digestive tract, and growth-correlated stages. Cranial ossification of the skull and development of the dentary apparatus is linked to the digestive system for ballan wrasse, and to their feeding habits—from preying on zooplankton to feeding on crustaceans and invertebrates on rocks and other substrates. As ballan wrasse is a nibbler, eating small meals, the digestive tract is short compared to the length of the fish, and it lacks a functional bulbus, a stomach, or peptic digestion. Furthermore, the liver and pancreas are important in the digestive process, displaying a larger relative volume of the digestive system than that in gastric teleosts.

ACKNOWLEDGMENTS

At UiB, we thank Prof. Harald Kryvi, Teresa Cieplinska, and Nina Ellingsen for help with dissecting fish and sectioning for studies of the digestive tract and at IMR Angela Etayo Ros for technical support. We also thank Thomas E. Berentsen and Espen Grøtan (Marine Harvest) for supplying the fish. We thank Dr. Hoang T.M.D. Le for input into writing an early version of ms. This work was funded by the Research Council of Norway, RCN (Project; Intestinal function and health of ballan wrasse. Grant #244170). IR also acknowledges sabbatical grants from the UiB, Meltzer Foundation, and RCN #311627. The funders had no role in the study design, data collection and analysis, decision to publish, or preparation of the manuscript.

CONFLICT OF INTEREST

The authors have no conflicts of interest to declare.

AUTHOR CONTRIBUTIONS

Planning and preparing the study: ØS, IR. *Implementation of the study*: SN, ØS. *Analysis*: SN, IR, ØS. *Writing of the draft version*: SN, ØS, IR. *Editing and final approval of the manuscript*: SN, IR, ØS.

DATA AVAILABILITY STATEMENT

The data that supports the findings of this study are available in the supplementary material of this article.

ORCID

Ivar Rønnestad https://orcid.org/0000-0001-8789-0197

REFERENCES

Al-Hussaini, A.H. (1949) On the functional morphology of the alimentary tract of some fish in relation to differences in their feeding habits: anatomy and histology. *Quarterly Journal Microscopical Science*, 90(2), 109–139.

Atukorala, A.D. & Franz-Odendaal, T.A. (2014) Spatial and temporal events in tooth development of *Astyanax mexicanus*. *Mechanisms of Development*, 134, 42–54. https://doi.org/10.1016/j.mod.2014.09.002

Baglole, C.J. (1997) *Development of the digestive system in larval yellowtail (Pleuronectes ferruginea) and winter flounder (Pleurnectes americanus)*. Master thesis, University of Prince Edward Island, Charlottetown.

Bilal, S., Lie, K.K., Dalum, A.S., Karlsen, O.A. & Hordvik, I. (2019) Analysis of immunoglobulin and T cell receptor gene expression in ballan wrasse (*Labrus bergylta*) revealed an extraordinarily high IgM expression in the gut. *Fish & Shellfish Immunology*, 87, 650–658. https://doi.org/10.1016/j.fsi.2019.02.007

Bisbal, G.A. & Bengtson, D.A. (1995) Development of the digestive tract in larval summer flounder. *Journal of Fish Biology*, 47, 277–291. https://doi.org/10.1111/j.1095-8649.1995.tb01895.x

Bjordal, Å. (1988) Cleaning symbiosis between wrasse (Labridae) and lice infested salmon (*Salmo salar*) in mariculture.In: *International Council for the Exploration of the Sea*. F:17.

Burggren, W.W. & Pinder, A.W. (1991) Ontogeny of cardiovascular and respiratory physiology in lower-vertebrates. *Annual Review of Physiology*, 53, 107–135. https://doi.org/10.1146/annurev.ph.53.030191.000543

Carr, E.M. & Motta, P.J. (2020) Tooth length and occlusion in four species of piscivorous fishes: getting a grip on prey. *Environmental Biology of Fishes*, 103(8), 903–912. https://doi.org/10.1007/s10641-020-00991-8

Castro, L.F.C., Goncalves, O., Mazan, S., Tay, B.H., Venkatesh, B. & Wilson, J.M. (2014) Recurrent gene loss correlates with the evolution of stomach phenotypes in gnathostome history. *Proceedings of the Royal Society B: Biological Sciences*, 281(1775), 9. https://doi.org/10.1098/rspb.2013.2669

Cavrois-Rogacki, T., Davie, A., Monroig, O. & Migaud, H. (2019) Elevated temperature promotes growth and feed efficiency of farmed ballan wrasse juveniles (*Labrus bergylta*). *Aquaculture*, 511. https://doi.org/10.1016/j.aquaculture.2019.734237

Cignoni, P., Callieri, M., Corsini, M., Dellepiane, M., Ganovelli, F. & Ranzuglia, G. (2008) MeshLab: an open-source mesh processing tool. In: *Eurographics Italian Chapter Conference* (pp. 129–136). Salerno, Italy: The Eurographics Association. http://www.meshlab.net

Clifton, K.B. & Motta, P.J. (1998) Feeding morphology, diet, and ecomorphological relationships among five Caribbean Labrids (Teleostei, *Labridae*). *Copeia*, 1998(4), 953–966. https://doi.org/10.2307/1447342

Costello, M.J. (2006) Ecology of sea lice parasitic on farmed and wild fish. *Trends in Parasitology*, 22(10), 475–483. https://doi.org/10.1016/j.pt.2006.08.006

Dipper, F.A., Bridges, C.R. & Menz, A. (1977) Age, growth and feeding in the ballan wrasse *Labrus bergylta* Ascanius 1767. *Journal of Fish Biology*, 11, 105–120.

Dunaevskaya, E., Amin, A.B. & Ottesen, O.H. (2012) Organogenesis of Ballan wrasse *Labrus bergylta* (Ascanius 1767) larvae. *Journal of Aquaculture Research & Development*, 3(5), 142. https://doi.org/10.4172/2155-9546.1000146

Falk-Petersen, I.B. (2005) Comparative organ differentiation during early life stages of marine fish. *Fish & Shellfish Immunology*, 19(5), 397–412. https://doi.org/10.1016/j.fsi.2005.03.006

Faustino, M. & Power, D.M. (2001) Osteologic development of the viscerocranial skeleton in sea bream: alternative ossification strategies in teleost fish. *Journal of Fish Biology*, 58(2), 537–572. https://doi.org/10.1111/j.1095-8649.2001.tb02272.x

Figueiredo, M., Morato, T., Barreiros, J.P., Afonso, P. & Santos, R.S. (2005) Feeding ecology of the white seabream, *Diplodus sargus*, and the ballan wrasse *Labrus berhylta*, in the Azores. *Fisheries Research*, 75(1–3), 107–119. https://doi.org/10.1016/j.fishres.2005.04.013

Gagnat, M.R., Wold, P.A., Bardal, T., Øie, G. & Kjorsvik, E. (2016) Allometric growth and development of organs in ballan wrasse (*Labrus bergylta* Ascanius, 1767) larvae in relation to different prey diets and growth rates. *Biology Open*, 5, 1241–1251. https://doi.org/10.1242/bio.017418

Gisbert, E., Piedrahita, R.H. & Conklin, D.E. (2004) Ontogenetic development of the digestive system in California halibut (*Paralichthys californicus*) with notes on feeding practices. *Aquaculture*, 232(1–4), 455–470. https://doi.org/10.1016/s0044-8486(03)00457-5

Gomes, A.S., Kamisaka, Y., Harboe, T., Power, D.M. & Rønnestad, I. (2014) Functional modifications associated with gastrointestinal tract organogenesis during metamorphosis in Atlantic halibut (*Hippoglossus hippoglossus*). *BMC Developmental Biology*, 14(11), 16. https://doi.org/10.1186/1471-213x-14-11

Govoni, J.J., Boehlert, G.W. & Watanabe, Y. (1986) The physiology of digestion in fish larvae. *Environmental Biology of Fishes*, 16(1–3), 59–77. https://doi.org/10.1007/BF00005160

Hamre, K., Nordgreen, A., Grotan, E. & Breck, O. (2013) A holistic approach to development of diets for Ballan wrasse (*Labrus bergylta*)—a new species in aquaculture. *PeerJ*, 1, e99. https://doi.org/10.7717/peerj.99

Hamre, K., Yúfera, M., Rønnestad, I., Boglione, C., Conceição, L.E.C. & Izquierdo, M. (2013) Fish larval nutrition and feed formulation: knowledge gaps and bottlenecks for advances in larval rearing. *Reviews in Aquaculture*, 5(suppl. 1), S26–S58. https://doi.org/10.1111/j.1753-5131.2012.01086.x

Hansen, T.W., Folkvord, A., Grotan, E. & Sæle, Ø. (2013) Genetic ontogeny of pancreatic enzymes in *Labrus bergylta* larvae and the effect of feed type on enzyme activities and gene expression. *Comparative Biochemistry and Physiology. Part B, Biochemistry & Molecular Biology*, 164(3), 176–184. https://doi.org/10.1016/j.cbpb.2012.12.001

Heath, M.R. (1992) Field investigations of the early life stages of marine fish. *Advances in Marine Biology*, 28, 1–174. https://doi.org/10.1016/s0065-2881(08)60039-5

Helland, S., Lein, I., Sæle, Ø., Lie, K., Kousoulaki, K.K., van Dalen, S.C.M. et al. (2014) Effects of feeding frequency on growth and gut health of ballan wrasse juveniles. In: *Production of ballan wrasse—science and practice* (pp. 83–89). Oslo, Norway: Fiskeri-og havbruksnæringens forskningsfond (FHF) – The Norwegian Seafood Reserach Fund.

Inui, Y., Yamano, K. & Miwa, S. (1995) The role of thyroid hormone in tissue development in metamorphosing flounder. *Aquaculture*, 135(1–3), 87–98. https://doi.org/10.1016/0044-8486(95)01017-3

Kamisaka, Y. & Rønnestad, I. (2011) Reconstructed 3D models of digestive organs of developing Atlantic cod (*Gadus morhua*) larvae. *Marine Biology*, 158(1), 233–243. https://doi.org/10.1007/s00227-010-1554-x

Kjørsvik, E., Flaten, S., Bardal, T. & Wold, P.A. (2014) The digestive system of juvenile ballan wrasse. In: *Production of ballan wrasse—science and practice* (pp. 80–82). Oslo, Norway: Fiskeri-og havbruksnæringens forskningsfond (FHF) – The Norwegian Seafood Reserach Fund.

Koelz, H.R. (2009) Gastric acid in Vertebrates. *Scandinavian Journal of Gastroenterology*, 27(sup193), 2–6. https://doi.org/10.3109/00365529209095998

Kortner, T.M., Overrein, I., Øie, G., Kjørsvik, E., Bardal, T., Wold, P.-A., et al. (2011) Molecular ontogenesis of digestive capability and associated endocrine control in Atlantic cod (Gadus morhua) larvae. *Comparative Biochemistry and Physiology Part A: Molecular & Integrative Physiology*, 160(2), 190–199. https://doi.org/10.1016/j.cbpa.2011.05.033

Le, H., Lie, K.K., Etayo, A., Rønnestad, I. & Sæle, Ø. (2021) Physical and nutrient stimuli differentially modulate gut motility patterns, gut transit rate, and transcriptome in an agastric fish, the ballan wrasse. *PLoS ONE*, 16(2), e0247076. https://doi.org/10.1371/journal.pone.0247076

Le, H.T.M.D., Lie, K.K., Giroud-Argoud, J., Rønnestad, I. & Sæle, Ø. (2019) Effects of cholecystokinin (CCK) on gut motility in the Stomachless fish Ballan wrasse (*Labrus bergylta*). *Frontiers in Neuroscience*, 13, 553. https://doi.org/10.3389/fnins.2019.00553

Le, H.T.M.D., Shao, X., Krogdahl, Å., Kortner, T.M., Lein, I., Kousoulaki, K. et al. (2019) Intestinal function of the stomachless fish, Ballan wrasse (*Labrus bergylta*). *Frontiers in Marine Science*, 6, 140. https://doi.org/10.3389/fmars.2019.00140

Lie, K.K., Torresen, O.K., Solbakken, M.H., Rønnestad, I., Tooming-Klunderud, A., Nederbragt, A.J. et al. (2018) Loss of stomach, loss of appetite? Sequencing of the ballan wrasse (*Labrus bergylta*) genome and intestinal transcriptomic profiling illuminate the evolution of loss of stomach function in fish. *BMC Genomics*, 19, 17. https://doi.org/10.1186/s12864-018-4570-8

Marques, C., Faustino, F., Bertolucci, B., Paes, M.D., Valentin, F.N. & Nakaghi, L.S. (2017) Structural and ultrastructural description of larval development in *Zungaro jahu*. *Zygote*, 25, 149–159. https://doi.org/10.1017/S0967199416000423

Micale, V., Garaffo, M., Genovese, L., Spedicato, M.T. & Muglia, U. (2006) The ontogeny of the alimentary tract during larval development in common pandora *Pagellus erythrinus* L. *Aquaculture*, 251(2–4), 354–365. https://doi.org/10.1016/j.aquaculture.2005.05.048

Mitra, A., Mukhopadhyay, P.K. & Homechaudhuri, S. (2015) Histomorphological study of the gut developmental pattern in early life history stages of featherback, *Chitala chitala* (Hamilton). *Archives of Polish Fisheries*, 23(1), 25–35. https://doi.org/10.1515/aopf-2015-0003

Mumford, S., Heidel, J., Smith, C., Morrison, J., MacConnell, B. & Blazer, V. (2007) *Fish histology and histopathology*. West Virginia, USA: US fish and wildlife Service's National Conservation Training Center.

Osse, J.W.M. & van den Boogaart, J.G.M. (1995) Fish larvae, development, allometric growth, and the aquatic environment. *ICES Marine Science Symposia*, 201, 21–34.

Ottesen, O., Karlsen, Å., Treasurer, J.W., Fitzgerald, R., Maguire, J., Rebours, C. et al. (2008) Ballan wrasse offer efficient, environmentally friendly sea lice control. *Global Aquaculture Advocate*, 11(6), 44–45.

Ottesen, O.H., Dunaevskaya, E. & Arcy, J. (2012) Development of *Labrus bergylta* (Ascanius 1767) larvae from hatching to metamorphosis. *Journal of Aquaculture Research & Development*, 3(3), 127. https://doi.org/10.4172/2155-9546.1000127

Parichy, D.M., Elizondo, M.R., Mills, M.G., Gordon, T.N. & Engeszer, R.E. (2009) Normal table of postembryonic zebrafish development: staging by externally visible anatomy of the living fish. *Developmental Dynamics*, 238(12), 2975–3015. https://doi.org/10.1002/dvdy.22113

Pelletier, D., Dutil, J.D., Blier, P. & Guderly, H. (1994) Relation between growth rate and metabolic organization of white muscle, liver and digestive tract in cod, *Gadus morhua*. *Journal of Comparative Physiology B*, 164, 179–190.

Piccinetti, C.C., Grasso, L., Maradonna, F., Radaelli, G., Ballarin, C., Chemello, G. et al. (2017) Growth and stress factors in ballan wrasse (*Labrus bergylta*) larval development. *Aquaculture Research*, 48(5), 2567–2580. https://doi.org/10.1111/are.13093

Potthoff, T. (1984). Clearing and staining techniques. In Moser, H.G., Richards, W.J., Cohen, D.M. & Fahay, M.P., Kendall, A.W. Jr and Richardson, S.L. (Eds.), *Ontogeny and systematics of fishes* (Vol. Special Publication 1, pp. 35–37). Lawrence, USA: Allen Press, American Society of Ichthyologists and Herpetologists.

Ray, A.K. & Ringø, E. (2014) The gastrointestinal tract of fish. In: Merrifield, D. & Ringø, E. (Eds.) *Aquaculture nutrition: gut health, probiotics and prebiotics*, First edition. West Sussex: John Wiley and Sons, Ltd.

Rønnestad, I., Kamisaka, Y., Conceição, L.E.C., Morais, S. & Tonheim, S.K. (2007) Digestive physiology of marine fish larvae: hormonal control and processing capacity for proteins, peptides and amino acids. *Aquaculture*, 268(1–4), 82–97. https://doi.org/10.1016/j.aquaculture.2007.04.031

Rønnestad, I., Yúfera, M., Ueberschär, B., Ribeiro, L., Sæle, Ø. & Boglione, C. (2013) Feeding behaviour and digestive physiology in larval fish: current knowledge, and gaps and bottlenecks in research. *Reviews in Aquaculture*, 5, S59–S98. https://doi.org/10.1111/raq.12010

Sæle, Ø., Haugen, T., Karlsen, O., van der Meeren, T., Baeverfjord, G., Hamre, K. et al. (2017) Ossification of Atlantic cod (*Gadus morhua*)—Developmental stages revisited. *Aquaculture*, 468, 524–533. https://doi.org/10.1016/j.aquaculture.2016.11.004

Sæle, Ø. & Pittman, K.A. (2010) Looking closer at the determining of a phenotype? Compare by stages or size, not age. *Journal of Applied Ichthyology*, 26(2), 294–297. https://doi.org/10.1111/j.1439-0426.2010.01424.x

Sæle, Ø., Solbakken, J.S., Watanabe, K., Hamre, K. & Pittman, K. (2003) The effect of diet on ossification and eye migration in Atlantic halibut larvae (*Hippoglossus hippoglossus* L.). *Aquaculture*, 220(1–4), 683–696. https://doi.org/10.1016/s0044-8486(02)00584-7

Sæle, Ø., Solbakken, J.S., Watanabe, K., Hamre, K., Power, D. & Pittman, K. (2004) Staging of Atlantic halibut (*Hippoglossus hippoglossus* L.) from first feeding through metamorphosis, including cranial ossification independent of eye migration. *Aquaculture*, 239(1–4), 445–465. https://doi.org/10.1016/j.aquaculture.2004.05.025

Sala, R., Santamaría, C.A. & Crespo, S. (2005) Growth of organ systems of *Dentex dentex* (L) and *Psetta maxima* (L) during larval development. *Journal of Fish Biology*, 66, 315–326. https://doi.org/10.1111/j.1095-8649.2005.00580.x

Sánchez-Amaya, M.I., Ortiz-Delgado, J.B., García-López, Á., Cárdenas, S. & Sarasquete, C. (2007) Larval ontogeny of redbanded seabream *Pagrus auriga* Valenciennes, 1843 with special reference to the digestive system. A histological and histochemical approach. *Aquaculture*, 263(1–4), 259–279. https://doi.org/10.1016/j.aquaculture.2006.10.036

Segner, H., Storch, V., Reinecke, M., Kloas, W. & Hanke, W. (1994) The development of functional digestive and metabolic organs in turbot, *Scophthalmus maximus*. *Marine Biology*, 119(3), 471–486. https://doi.org/10.1007/BF00347544

Skiftesvik, A.B., Bjelland, R.M., Durif, C.M.F., Johansen, I.S. & Browman, H.I. (2013) Delousing of Atlantic salmon (*Salmo salar*) by cultured vs. wild ballan wrasse (*Labrus bergylta*). *Aquaculture*, 402, 113–118. https://doi.org/10.1016/j.aquaculture.2013.03.032

Smith, D.M., Grasty, R.C., Theodosiou, N.A., Tabin, C.J. & Nascone-Yoder, N.M. (2000) Evolutionary relationships between amphibian, avian and mammalian stomachs. *Evolution & Development*, 2(6), 348–359. https://doi.org/10.1046/j.1525-142x.2000.00076.x

St John, M.E., Holzman, R. & Martin, C.H. (2020) Rapid adaptive evolution of scale-eating kinematics to a novel ecological niche. *The Journal of Experimental Biology*, 223(Pt 6), jeb217570. https://doi.org/10.1242/jeb.217570

Valen, R., Eilertsen, M., Edvardsen, R.B., Furmanek, T., Rønnestad, I., van der Meeren, T. et al. (2016) The two-step development of a duplex retina involves distinct events of cone and rod neurogenesis and differentiation. *Developmental Biology*, 416(2), 389–401. https://doi.org/10.1016/j.ydbio.2016.06.041

Van der Heyden, C., Allizard, F., Sire, J.Y. & Huysseune, A. (2005) Tooth development in vitro in two teleost fish, the cichlid *Hemichromis bimaculatus* and the cyprinid *Danio rerio*. *Cell and Tissue Research*, 321(3), 375–389. https://doi.org/10.1007/s00441-004-1036-x

Wallace, K.N., Akhter, S., Smith, E.M., Lorent, K. & Pack, M. (2005) Intestinal growth and differentiation in zebrafish. *Mechanisms of Development*, 122(2), 157–173. https://doi.org/10.1016/j.mod.2004.10.009

Wold, P.A. (2007). *Functional development and response to dietary treatment in larval Atlantic cod (Gadus morhua L.)*. Doctoral thesis, NTNU Norwegian University of Science and Technology, Trondheim, NTNU Norwegian University of Science and Technology, Trondheim, Norway.

Yamano, K., Tagawa, M., DeJesus, E.G., Hirano, T., Miwa, S. & Inui, Y. (1991) Changes in whole-body concentrations of thyroid-hormones and cortisol in metamorphosing conger eel. *Journal of Comparative Physiology B: Biochemical, Systemic, and Environmental Physiology*, 161, 371–375. https://doi.org/10.1007/BF00260795

Yúfera, M. & Darías, M.J. (2007) The onset of exogenous feeding in marine fish larvae. *Aquaculture*, 268(1–4), 53–63. https://doi.org/10.1016/j.aquaculture.2007.04.050

Zambonino Infante, J.L. & Cahu, C. (2001) Ontogeny of the gastrointestinal tract of marine fish larvae. *Comparative Biochemistry and Physiology Part C*, 130(4), 477–487. https://doi.org/10.1016/S1532-0456(01)00274-5

Zambonino Infante, J.L. & Cahu, C.L. (1994) Influence of diet on pepsin and some pancreatic enzymes in sea bass (*Dicentrarchus labrax*) larvae. *Comparative Biochemistry and Physiology*, 109A(2), 209–212. https://doi.org/10.1016/0300-9629(94)90122-8

Zambonino Infante, J.L., Gisbert, E., Sarasquete, C., Navarro, I., Gutierrez, J. & Cahu, C.L. (2008) Ontogeny and physiology of the digestive system of marine fish larvae. In: Cyrino, J.E.P., Bureau, D.P. & Kapoor, B.G. (Eds.) *Feeding and digestive functions of fishes*. Enfield, USA: Science Publishers, pp. 281–348.

Zhou, W., Krogdahl, A., Saele, O., Chikwati, E., Lokka, G. & Kortner, T.M. (2021) Digestive and immune functions in the intestine of wild Ballan wrasse (*Labrus bergylta*). *Comparative Biochemistry and Physiology. Part A, Molecular & Integrative Physiology*, 260, 111011. https://doi.org/10.1016/j.cbpa.2021.111011

SUPPORTING INFORMATION

Additional supporting information may be found in the online version of the article at the publisher's website.

How to cite this article: Norland, S., Sæle, Ø. & Rønnestad, I. (2022) Developmental stages of the ballan wrasse from first feeding through metamorphosis: Cranial ossification and the digestive system. *Journal of Anatomy*, 241, 337–357. Available from: https://doi.org/10.1111/joa.13686